NASA CR-178029

Design and Verification by Nonlinear Simulation of a Mach/CAS Control Law for the NASA TSRV B-737 Aircraft

Final Report

Kevin R. Bruce

Boeing Commercial Airplane Company
Seattle, Washington

Prepared for
NASA TSRV
Contract NAS1-14880

National Aeronautics and
Space Administration

August 1986

NASA CR-178029

Design and Verification by Nonlinear Simulation of a Mach/CAS Control Law for the NASA TSRV B-737 Aircraft

Final Report

Kevin R. Bruce

Boeing Commercial Airplane Company
Seattle, Washington

TABLE OF CONTENTS

1.0 SUMMARY

A Mach/CAS control law was designed and developed for use on the NASA Terminal System Research Vehicle (TSRV) B737 aircraft to conduct research in profile descent procedures and approach energy management. The system operates by using the elevator to control speed; the throttle position being fixed.

The control law was designed primarily using linear analysis techniques, although a nonlinear feedforward term was included in the system to improve response to a ramp input. The system was modeled on a nonlinear aircraft simulator to confirm the original linear design and validate the system design at additional flight conditions.

The system satisfied all the design requirements for gain and phase margin, transient speed target overshoot, speed holding in wind shear, and elevator activity in turbulence.

2.0 INTRODUCTION

This report documents the design and performance analysis of a Mach/CAS control law for implementation on the NASA TSRV B737 aircraft. The law is designed to enable NASA to perform approach energy management research. For example, on starting descent to an airport, the pilot switches the autopilot from a straight level flight mode to a constant Mach descent mode. As the aircraft descends, air density increases and thus CAS increases. At some preselected value of CAS, the autopilot switches from Mach hold mode to CAS hold mode and continues descending. The Mach, CAS commands, and the switching point may have been determined by an energy management computer to satisfy target objectives of distance versus altitude, speed, and time of arrival.

The system operates by using the elevator to control speed. The throttle normally would be set at idle thrust, although other settings may be selected to allow for operational considerations (e.g., pressurization or anti-icing considerations).

The report details the linear design results and describes modifications made to the basic design to improve performance for ramp input demands and in wind shear conditions. Consideration is given to a practical implementation yielding transient free switching between Mach and CAS mode and also to minimize modification to the existing aircraft.

The preferred design configuration was implemented on a nonlinear aircraft simulator at the Boeing Renton Flight Simulation Center. The nonlinear simulation was used to confirm the original design results and validate the design at additional flight conditions.

3.0 SYMBOLS

K_{V_2}	Actuator gain (scheduled)
α	Angle of attack (deg)
V_{CAS}	Calibrated airspeed (kn)
V_{CAS_E}	Calibrated airspeed error (kn)
θ_{cmd}	Commanded attitude
$V_{CAS_{CMD}}$	Commanded calibrated airspeed (kn)
$Mach_{CMD}$	Commanded Mach number
$V_{T_{CMD}}$	Commanded true airspeed (kn)
δ_{e_c}	Commanded elevator deflection
F	Conversion factor (CAS to TAS)
Mach	Current measured Mach number
ζ	Damping ratio
ϕ_{ug}	Dryden wind spectrum (longitudinal gusting)
ϕ_{wg}	Dryden wind spectrum (vertical gusting)
δ_e	Elevator deflection (deg)
V_e	Equivalent airspeed (kn)
V_{CLIM}	Feedforward rate limit
q_F	Filtered pitch rate (deg/s)
V_{wo}	Filtered velocity (kn)
γ	Flightpath angle
K_θ, K_q, K_F	Gains (fixed)
V_{GT}	Groundspeed (kn)
V_{mwic}	Initial condition for wind velocity (kn)
$\dot{V}$	Inertial acceleration of airplane (kn/s)
V	Inertial velocity of airplane (kn)

K_x	Integrator gain
U_g	Longitudinal gust (m/s)
H	Nominal height (m)
h	Perturbed height (m)
$q,\dot{\theta}$	Pitch rate (rad/s)
θ	Pitch angle (rad)
σ_u	RMS longitudinal gust level (m/s)
σ_w	RMS vertical gust velocity (m/s)
a	Speed of sound
$Mach_{switch}$	Switch velocity (CAS to Mach)
$V_{CAS_{switch}}$	Switch velocity (Mach to CAS) (kn)
τ_v	Time constant for complementary filter (sec)
V_T	True airspeed (kn)
$V_{T_{CMD}}$	True airspeed command (kn)
V_{T_E}	True airspeed error
K_{V_1}	Velocity error gain
u	Velocity of airplane in longitudinal axis
W_g	Vertical gust (m/s)
V_{MW}	Wind shear magnitude (kn)
F_{HWS}	Wind shear scaling factor (horizontal) (m)
Lu, Lw	Wind turbulence characteristic lengths (longitudinal and vertical)
V_{wind}	Wind velocity (kn)

ACRONYMS

ACSL	Advanced continuous simulation language
ATOPS	Advanced transport operating systems
CAS	Calibrated airspeed
RFSL	Renton Flight Simulation Laboratory
TAS	True airspeed

4.0 DESIGN AND PERFORMANCE REQUIREMENTS

To ensure satisfactory performance of the final control law, the following design and performance requirements were imposed on the design. The control law must:

1. Be suitable for use at all flight conditions and throttle settings.
2. Be implemented with minimum modification to the existing autopilot design (refs. 1 through 4) commensurate with meeting all stability and performance requirements.
3. Maintain approximately constant transient response performance at all flight conditions with a speed control bandwidth equal to or greater than 0.05 r/s.
4. Provide satisfactory damping (approximately $\zeta = 0.7$) on dominant roots at all flight conditions and demonstrate insensitivity in damping and bandwidth to 10% variations in nominal gains.
5. Limit overshoots in indicated airspeed to within 2 kn for step inputs; maintain indicated airspeed to within 2 kn for a ramp input of 1 ft/s^2. For wind shear of 1 kn/s the maximum error in airspeed should not exceed 10 kn and the steady state error should be zero.
6. Maintain gain and phase margins equal to or greater than 6 dB and 60 deg, respectively.
7. Elevator activity should not be greater than comparable existing control systems.

The Mach/CAS control system can be considered to consist of two control loops (fig. 1):

1. An outer velocity hold loop using true airspeed (V_T) and acceleration ($\dot{v}$) feedback.

The reference input, either Mach or CAS command, is converted to a true airspeed command that drives the outer (velocity hold) loop. As the Mach/CAS conversion is outside the control loop, the linear analysis is restricted to considering the attitude loop and the true airspeed control loop.

The reason for converting to true airspeed instead of controlling CAS or Mach directly is that this approach requires only one control law. Also, true airspeed is compatible with inertial acceleration feedback, which is used to provide damping of the velocity loop. This way, approximately constant inner loop dynamics are achieved over the entire flight envelope without the need for outer loop gain programmers.

The practical implementation of generating the true airspeed command from either CAS or Mach is considered in a later section of this report.

The design of the control law was accomplished by first considering the inner attitude loop in isolation (i.e., θ and q feedback only). An attitude control loop was designed that gave suitable performance over the whole flight regime. Next, the velocity loop was added and the performance of the overall loop optimized.

4.1 INNER AUTOPILOT LOOP

The inner autopilot loop (fig. 2) was modeled using a gain (KV_2) and a first-order lag at 20 rad/s to represent the elevator actuator. The q feedback was obtained from the baseline control system and was prefiltered through a 16 rad/s washout filter and scaled in deg/s. The washout filter originally was added to eliminate steady state biases on pitch rate feedback.

The inner autopilot loop was designed to give approximately constant performance in terms of bandwidth and transient response. The three cases selected for examination were considered representative of the whole flight envelope. They consisted of:

1. High speed: CAS = 320 kn, H = 6100m, flaps = 0 deg
2. Mid speed: CAS = 250 kn, H = 3048m, flaps = 0 deg
3. Low speed: CAS = 120 kn, H = 500m, flaps = 40 deg

In the current aircraft design, the forward path gain K_{V_2} is preprogrammed to vary with V_{CAS} from 1.0 at 120 kn to 0.275 at 360 kn (fig. 3). It was considered desirable to maintain this gain scheduling.

Root locus techniques were used to examine the low-speed and high-speed performance and determine acceptable values for K_θ and K_q. Table 1 shows the dominant complex roots for the nominal low-speed gain values $K_\theta = 8$ and $K_q = 5.16$.

Speed	ω(r/s)	ζ
Low (120 kn)	9.27	0.98
Mid (250 kn)	16.0	0.6
High (320 kn)	15.9	0.6

Table 1. Inner Loop Dominant Complex Roots for Nominal Gains

The root loci for the low-speed case is shown in Figure 4 for gain variations of K_θ and K_q around their nominal values. It can be seen that the system is well damped for large variations in gains K_θ, K_q ($\pm 30\%$). The corresponding root locus plot at high speed (fig. 5) shows lower damping ($\zeta = 0.6$); however, the system is not sensitive to gain variation of $\pm 10\%$. The transient response at high and low speed (for a step change in pitch command, θ_{cmd}) was considered satisfactory (fig. 6). The rise time (time of 63% of final value) was 0.8 sec compared with 0.75 sec at low speed.

A summary of the design results for the inner autopilot loop is shown in Table 2. The table includes the design results achieved for the mid-speed case. The minimum gain and phase margins were 23 dB and 82 deg respectively for the three cases considered. A typical open loop frequency response is shown in Figure 7 (low-speed condition).

	K_{V_2}	Gains K_q	K_θ	Rise time (sec) to 63%	Settling time (sec) to 95%	(r/s)		Gain margin (dB)	Phase margin (deg)
						(3dB)	(90 deg)		
High speed (320 kn)	0.426	5.16	8	0.80	3.05	1.0	4.5	23.5	95.2
Mid speed (250 kn)	0.6	5.16	8	0.75	2.6	1.2	4.8	23.3	91.1
Low speed (120 kn)	1.0	5.16	8	0.75	2.25	1.65	3.0	23.3	82.0

Table 2. Inner Autopilot Loop Performance

4.2 VELOCITY HOLD LOOP

The basic velocity hold loop (fig. 8) was designed with the same objectives as for the inner autopilot loop (i.e., to minimize gain variation and give similar transient performance over the whole flight regime). A summary of the results for the three speed cases is given in Table 3 for $K_\theta = 8$, $K_q = 5.16$, $K_{V_1} = 0.1$, $K_x = 0.35$. The dominant complex roots are shown in Table 4.

	Rise time (sec) to 63%	Settling time (sec) to 95%	(r/s)		Gain margin (dB)	Phase margin (deg)
			(3 dB)	(90 deg)		
High speed (320 kn)	12.5	19.5	0.175	0.142	13.8	65.5
Mid speed (250 kn)	12.5	19.5	0.18	0.15	12.2	66.3
Low speed (120 kn)	15.0	39.0	0.09	0.13	18.9	75.9

Table 3. Outer Loop Performance

Speed	ω(r/s)	ζ
Low (120 kn)	0.33	0.72
Mid (250 kn)	0.25	0.62
High (320 kn)	0.23	0.70

Table 4. Outer Velocity Hold Loop Dominant Complex Roots for Nominal Gains

Considering the low-speed case the rise time (to 63% of final value) was 15.0 sec (fig. 9). Adequate gain and phase margins of 18.9 dB and 75.9 deg, respectively, were obtained (fig. 10) and the system closed loop bandwidth (to the 90 deg phase shift point) was 0.16 r/s (fig. 11).

The root locus plots show the system sensitivity to gain variations of 50%, and it can be seen that the damping of the dominant complex pole (speed control) is sufficiently insensitive to gain variations (figs. 12 and 13).

In the high-speed case, the rise time to 63% had decreased to 12.5 sec (fig. 14). Stability margins were again more than adequate at 13.8 dB and 65.5 deg, respectively (fig. 15). The root loci of the dominant complex poles are shown in Figure 16 together with the line of constant damping for $\zeta = 0.7$. The diagrams show the insensitivity of the system dynamics to gain variation.

Results at mid speed were very similar to the high-speed case for both the transient and frequency response (table 4).

It was considered desirable to restrict the maximum vertical acceleration to 0.1 g_n. It can be seen from Figure 17 that a 1-kn step velocity command (high-speed case) gave a maximum vertical acceleration of -0.32 kn/s (-0.017 g_n). Hence, a 6-kn change in input would just exceed the 0.1 g_n criterion. A limiter on airspeed error was included to overcome this problem.

5.0 DESIGN OF NONLINEAR FEEDFORWARD TERM

The control law described previously, gave good performance to commanded step changes in velocity. However, it resulted in poor performance for a ramp input (i.e., constant acceleration demand). A 0.6 kn/s (1 ft/s) ramp input produced a steady state velocity error of 6 kn (fig. 18), whereas the design requirement allows 2 kn for this condition.

This problem could be solved by using one of two methods:

1. Additional forward path integrator.
2. Nonlinear feedforward term.

The second method, the nonlinear term, avoided the possibility of stability problems and was considered a simpler option to implement practically.

The feedforward term consisted of essentially a differentiator followed by a rate limited lag. For implementation purposes, the differentiator was modeled by a gain and a high-pass filter (washout filter) having a small time constant compared with the bandwidth of the velocity hold loop. As the dominant loop time constant was 5 sec, a time constant at least ten times smaller was required and a value of 0.1 sec was nominally selected. This derivative term can be added to the control system error signal and can be interpreted as a shaped command input.

Consider the action of the derivative term alone (fig. 19), that is, one without any rate limiter or lag, then for a ramp input, the output from the differentiator is a step. By selection of the appropriate gain, the addition of this signal to the loop error signal drives the system to null the velocity error due to the ramp input (fig. 20).

However, for a step input, the output of the differentiator is an impulse, and the addition of this signal to the loop error signal causes an undesirable overshoot in the system response (fig. 21).

A solution to the problem is the introduction of a nonlinear element, namely a lag having a rate limit (V_{CLIM}) (fig. 22). This has the effect of severely attenuating the feedforward impulse response for a step command in velocity. It can be seen in Figure 23 that lowering the limit reduces the overshoot on the step response such that for $V_{CLIM} \leq 0.6$ kn/s, the response approximates the step response for the baseline system without the feedforward term.

With a ramp input, the output from the differentiator is a step, and the rate limited lag only affects the settling time of the lag. For $K_F = 10.8$ and washout filter time constant of 0.1, the feedforward gain is approximately 1. Therefore, for a ramp input of 0.6 kn/s, the limit only affects the ramp response for value of $V_{CLIM} < 0.6$ kn/s. This is verified in Figure 24 which shows the same ramp response for $V_{CLIM} \geq 0.6$ and $V_{CLIM} = 0.06$.

The results presented above were carried out at high (V_{CAS} = 320 kn, H = 6100m) and the gain K_F was optimized to null the error in TAS (K_F = 10.8). However, at low speed the optimum response was obtained with the gain K_F = 15. This is due to the fact that for the same input (whether step or ramp), the response of the feedback terms V_T and $\dot{v}$ is not identical over the whole flight envelope, whereas, obviously the feedforward term is the same. Rather than have gain scheduling, a compromise value of gain was selected (K_F = 13.0) that gave acceptable performance over the whole aerodynamic range. Maximum error to ramp input of 0.6 kn/s was within ±2 kn for both the high- and low-speed cases (figs. 25 and 26).

6.0 WIND SHEAR AND TURBULENCE

The effect of wind shear and turbulence on the control law was investigated using transient and frequency response techniques.

For the control system in Figure 8, a wind shear of 1 kn/s gave rise to 10 kn steady state error in airspeed (fig. 27). This system used inertial acceleration to provide the derivative feedback of velocity. Good tracking of wind shear without the standoff error could be obtained by feeding back the derivatives of airspeed. However, this would result in excessive elevator activity in turbulent situations. The addition of a complementary filter in the derivative feedback path allows a compromise to be made between the maximum transient airspeed error in a wind shear situation and the elevator activity experienced in turbulence. The complementary filter consists of:

(1) Differentiating and low-pass filtering the airspeed signal. This gives long-term derivative feedback of airspeed and eliminates the standoff error. The turbulence component is filtered to reduce elevator activity.

(2) High-pass (or washout) filtering the inertial acceleration signal and adding the signal to the airspeed signal. The two signals complement each other giving a unity transfer function. The high-frequency component of the inertial signal is comparatively free of noise.

The implementation of this filter is shown in Figure 28. The maximum airspeed error in a wind shear and the time required for the error in airspeed to reduce to zero are a function of the time constant τ_V. However, the penalty for reducing the effect of wind shear is an increase in the elevator activity due to turbulence. The relationships between elevator activity and maximum CAS error are shown in Figure 29 for a Dryden turbulence spectrum (ref. 5) with an rms level of 0.3 m/s (combined horizontal and vertical).

As the control law is not to be used for final approach, then the performance criterion in wind shear is not severe (i.e., 10 kn max error for 1 kn/s wind shear). The second constraint considered was that of elevator activity, which should not be worse than results obtained with the existing TSRV aircraft. As the airplane does not have a velocity hold mode that uses the elevator, then results were taken from turbulence results for the TSRV glideslope control law. The airplane does have this mode but not using elevator. Although the results were not directly comparable, they provided a guide to the levels of elevator activity that were acceptable.

From Figure 29, an initial value of τ_V = 10 sec was taken. For this system, the effect of turbulence was determined by modeling the wind using the Dryden spectrum for horizontal and vertical and evaluating the rms elevator activity. The results of vertical and longitudinal turbulence of 1.5 m/s rms are shown in Table 5 below. When compared with the results for the glideslope track law, the level of elevator activity was considered acceptable.

	Low-speed elevator	Activity (deg rms)
	Velocity hold law	Glideslope track law
Vertical gusts (1.5 m/s rms)	1.4	1.56
Longitudinal gusts (1.5 m/s rms)	0.5	0.835

Table 5. The rms Elevator Activity Due to Turbulence

The effect of the complementary filter (τ_V = 10 sec) on the frequency response of the elevator in longitudinal turbulence can be seen in Figure 30. Above approximately 0.3 r/s, the complementary filter raises the frequency response by approximately 7 dB; however, this was considered acceptable. At low speed (fig. 31), the increase in the frequency response caused by the addition of the filter was not significant above 0.1 r/s. However, below 0.03 r/s the filter reduced the sensitivity to gust, i.e., improved performance to wind shear.

In the case of vertical turbulence, the effect on the elevator activity of including the complementary filter was not significant (fig. 32) for both the high and low speed.

The effect of the complementary filter on the response of airspeed error for longitudinal turbulence can be seen in Figure 33. The filter has the effect of reducing the sensitivity to wind shear (i.e., low-frequency sensitivity) without significantly increasing the sensitivity to turbulence.

The sensitivity of the airspeed error to vertical turbulence was not significantly affected by the inclusion of the filter in both the high- and low-speed cases (fig. 34).

7.0 IMPLEMENTATION OF MACH/CAS HOLD

7.1 CONVERSION TO TRUE AIRSPEED

Consideration has been given to the method of converting from CAS and Mach to true airspeed, which is used in the control law. Figure 1 shows a simplified block diagram of the control system using a true airspeed command ($V_{T_{CMD}}$) and true airspeed (V_T) feedback to form the error signal

$$V_{T_E} = V_{T_{CMD}} - V_T \tag{1}$$

It is possible to compute $V_{T_{CMD}}$ from the pilot selected $V_{CAS_{CMD}}$ using a conversion formula. However, the conversion formula is complex and requires accurate measurement of several parameters. The risk of incurring a significant error in $V_{T_{CMD}}$ is therefore substantial. Such an error would cause an equivalent standoff between the selected $V_{CAS_{CMD}}$ and the actual V_{CAS}. This approach is therefore unacceptable. However, this problem can be eliminated by implementing the control loop in terms of the error in V_{CAS}.

$$V_{CAS_E} = V_{CAS_{CMD}} - V_{CAS} \tag{2}$$

and conversion of this error signal into the equivalent true airspeed error signal

$$V_{T_E} = F.V_{CAS_E} \tag{3}$$

In this case, a less accurate conversion factor (derived from speed conversion tables) will suffice.

$$F = \frac{1}{(1 - 0.394 \times 10^{-4}h)} \tag{4}$$

where h is in m. As V_{T_E} is controlled to zero, so V_{CAS_E} must go to zero, and an exact measurement of h is not critical to accurately controlling V_{CAS}.

In the Mach hold control loop, the accuracy problem can be avoided. Restating Equation 1 above

$$V_{T_E} = V_{T_{CMD}} - V_T$$

then $V_{T_{CMD}}$ can be obtained from $V_{T_{CMD}} = Mach_{CMD} \cdot a$

where a = speed of sound and $Mach_{CMD}$ = commanded Mach number.

therefore

$$V_{T_{CMD}} = \frac{Mach_{CMD} \cdot V_T}{Mach} \tag{5}$$

where Mach = Current Mach number.

$$V_{T_E} = \frac{Mach_{CMD}}{Mach} \cdot V_T - V_T \tag{6}$$

$$V_{T_E} = \left(\frac{Mach_{CMD}}{Mach} - 1\right) V_T \tag{7}$$

It can be seen that errors in measuring V_T will not cause steady state errors in Mach hold. As Mach tends to $Mach_{CMD}$, so V_{T_E} tends to zero. The implementation of the equations discussed above is shown in Figure 35.

7.2 CONTROL LAW INITIAL CONDITIONS

During the first section of descent, the control system is designed to hold the aircraft at constant Mach. When CAS equals a preselected CAS, then the system automatically switches to CAS hold and continues the descent by maintaining constant CAS. On ascent, the reverse is true. The control law initially is designed to maintain constant CAS, and at a preselected Mach, the system switches to holding constant Mach.

In order to minimize transients on switching between the two modes of operation, it is necessary to set

$$V_{CAS_{CMD}} = V_{CAS} \tag{8}$$

when in the Mach hold mode (in descent), and switch to CAS hold when

$$V_{CAS} = V_{CAS_{SWITCH}} \tag{9}$$

Similarly, when the airplane is climbing and in the CAS mode, the Mach command should be set to the current value, i.e.:

$$Mach_{CMD} = Mach \tag{10}$$

and the system switched to Mach hold when

$$Mach = Mach_{SWITCH} \tag{11}$$

An additional important consideration is that the forward loop integrator should be held at its current value (clamped) if the elevator limits during flight. The integrator should be "unclamped" when the elevator comes of the limit or the input to the integrator changes sign.

8.0 VALIDATION OF RESULTS

The equations describing the Mach/CAS control law were implemented on a nonlinear aircraft simulator. This was considered desirable in order to:

1. Validate the design results obtained using linear analysis design techniques and results obtained using a simplified nonlinear model with linear aerodynamics (ACSL Simulation (ref. 6)).
2. Examine the noise free performance at other flight conditions not covered by the linear analysis.
3. Demonstrate the ability to provide transient free switching from Mach hold to CAS hold and vice versa.
4. Confirm the performance of the system in wind shear and turbulent conditions.

8.1 NOISE FREE RESULTS

Initially, the free airplane responses obtained using the ACSL program were compared with the results obtained with nonlinear aircraft simulation.

The ACSL simulation used derivatives obtained at two flight conditions namely:

1. Low speed: V_{CAS} = 120 kn, H = 500m, γ = 0, and flaps = 40 deg
2. High speed: V_{CAS} = 320 kn, H = 6100m, γ = 0, and flaps = 0 deg

Simulation runs were carried out at these conditions with an initial offset of 1 deg from trimmed condition. Figure 36a shows plots of θ and α for the linear simulation at the low-speed conditions and Figure 36b shows the nonlinear simulator results for θ and α.

It can be seen that the ACSL simulation gave a phugoid oscillation of 37 sec compared with 42 sec with the nonlinear simulator. The short period response of α crossed the trimmed steady state value at 1.6 sec and 4.0 sec (for the linear system) compared with 2.0 sec and 4.5 sec for the nonlinear aircraft simulation.

At high-speed, the linear system took 106 sec (fig. 37a) for the phugoid oscillation compared with 82 sec (fig. 37b) for the nonlinear aircraft simulation. The short period crossing points (α response) occurred at 0.64 and 1.8 for the ACSL system and 0.7 and 2.2 for the nonlinear aircraft simulation model.

A detailed comparison of the B-737 aerodynamics on the nonlinear aircraft simulation was not possible within the time scale available. However, the discrepancy between the ACSL and nonlinear aircraft simulation was acceptable considering the difference in the levels of sophistication between the two models.

To confirm the validity of the overall control law, the time response to step change in true airspeed was examined. Figure 38a shows that for the linear model at high speed, it took 20 sec to achieve 95% of the steady state value compared with 18 sec for the nonlinear aircraft simulation result. At low speed, the 95% level was achieved after 36.8 sec using the ACSL simulation (fig. 38b) and 35 sec with the nonlinear aircraft simulation. This small discrepancy in the models was considered acceptable and could be explained by differences in the aerodynamics and by the additional complexity and nonlinear elements of the nonlinear aircraft simulation.

small discrepancy in the models was considered acceptable and could be explained by differences in the aerodynamics and by the additional complexity and nonlinear elements of the nonlinear aircraft simulation.

A disadvantage of the linear simulation was its restriction to a limited number of flight conditions. The addition of extra flight conditions would require extensive modification to the program. However, the nonlinear aircraft simulation allowed the performance of the system to be determined at other flight conditions, namely:

1. CAS = 350 kn, H = 6100m, flaps 0 deg
2. CAS = 250 kn, H = 6100m, flaps 0 deg
3. CAS = 200 kn, H = 3048m, flaps 0 deg
4. CAS = 160 kn, H = 500m, flaps 15 deg

The response to a step change in true airspeed at these flight conditions is shown in Figure 39. It can be seen that the performance is within the design requirements for all conditions.

In addition to the step response, the effect of a ramp input (0.3 m/s^2) was examined. In order to achieve a similar response at both high and low speed compared with the ACSL results, a feedforward gain (K_F) of 6.5 was selected (figs. 40 and 41) compared with linear design requirement of 13.0 (figs. 25 and 26).

A primary requirement of the system is that it should provide transient free switching between the Mach and CAS hold mode. This is demonstrated in Figure 42, which shows an aircraft descent from approximately 6700m, at a rate of -7.6 m/s. The Mach hold mode has been selected so that initially the system captures and holds Mach = 0.7. When holding Mach number and descending, CAS increased. The simulation stopped when CAS was 324.7 kn, although the measured value tended toward the requirement of 325 kn. Maximum transient error at switchover was less than 1 kn.

Transient free switching between CAS and Mach numbers was also demonstrated. For example, Figure 43 shows the effect of Mach and CAS for an aircraft climbing from 6100m at an initial nominal climb rate of 7.6 m/s. Initially, the control system is in the CAS hold mode, maintaining 300 kn while Mach number increases. At Mach = 0.68, the Mach hold mode automatically is switched in and the system holds Mach with a transient at switchover of less than Mach 0.003.

8.2 PERFORMANCE IN WIND SHEAR AND TURBULENCE

Figure 44 shows the results of the ACSL simulation for a horizontal wind shear of 1 kn/s plotted in terms of Mach response. Peak error in terms of airspeed was 7 kn and the error was reduced to 10% of its peak value by 38 sec. Figure 44 also shows the results of the nonlinear simulation, which gives approximately the same peak error and settling time as the ACSL simulation.

To determine the effect of wind shear at low speed, a wind shear profile was selected. The wind velocity is given by the equation:

$$V_{MW} = FHWS \cdot V_{MWIC}$$

where FHWS is a scaling factor dependent on height (fig. 45) and V_{MWIC} is an initial condition

for wind velocity set to 1 kn. The velocity error (V_{CAS_E}) is shown in Figure 46 for an aircraft climbing at a nominal 7.6 m/s. It can be seen that the maximum error in CAS was 0.32 kn.

In addition to wind shear, the effect of turbulence was examined at high and low speed. A Dryden wind spectrum (ref. 5) was selected, which is defined as

$$\phi_{u_g}(\gamma) = \frac{2\,\sigma_u^2 Lu}{(\,(1+(L_u\gamma)^2)}$$

for longitudinal gusting, and

$$\phi_{w_g}(\gamma) = \frac{\sigma_w^2\ Lw\ (1+3(Lw\gamma)^2)}{\pi\ (1+(Lw\gamma)^2)^2}$$

where Lu, Lw are the characteristic lengths

σ_u, σ_w are the rms gust velocity

and γ = w/v.

Typical values of scale length and rms level were selected, i.e., Lu, Lw = 183m; σ_u, σ_w = 1.5m rms. A typical plot of gust is shown in Figure 47; the rms level for the 100 sec sample was 1.4m. The effect of turbulence on the elevator is shown in Figure 48.

A summary of the results is shown in Table 6. For a medium level of turbulence (1.5m rms) the elevator response was considered acceptable.

	Longitudinal	Vertical
Inputs rms (m/s)	1.38*	1.38*
Elevator rms response (deg)	0.26	0.7
Velocity rms response (kn)	2.83	0.47

* Calculated for 100 sec time history.

Table 6. Summary of Turbulence Results

9.0 CONCLUSIONS

1. A Mach/CAS hold control system was designed using linear analysis techniques for flight conditions.
   - High speed: CAS = 320 kn, H = 6100m, γ = 0, flaps = 0 deg
   - Mid speed: CAS = 250 kn, H = 3048m, γ = 0, flaps = 0 deg
   - Low speed: CAS = 120 kn, H = 500m, γ = 0, flaps = 40 deg

2. The basic design was modified—
   - To improve performance in wind shear by the addition of a complementary filter in the feedback path.
   - To improve the response to a ramp input by the inclusion of a nonlinear feedforward term.

2. The basic design was modified—
   - To improve performance in wind shear by the addition of a complementary filter in the feedback path.
   - To improve the response to a ramp input by the inclusion of a nonlinear feedforward term.

3. For the design cases considered, the system satisfied the design criteria.
   - The minimum gain and phase margins were 12 dB and 65 deg.
   - The rise time (to 63% of final value) for a step input was 13.5 sec ± 11%.
   - The overshoot to a step input was less than 2 kn.
   - The peak error in airspeed, due to a 1 kn/s wind shear, was less than 10 kn. The error reduced to zero in the steady state.
   - Elevator activity was less than 1.5 deg rms for vertical gusts of 1.5 m/s rms.
   - For a ramp input of 1 kn/s^2, the error in airspeed was less than 2 kn.

4. Consideration was given to practical implementation in order to provide transient free switching between the Mach and CAS hold modes. The system has been designed to be implemented with minimum modification to the existing design.

5. The control system was implemented on the nonlinear aircraft simulator, which enabled simulation runs to be made at several flight conditions not covered in the linear design, namely:
   - CAS = 160 kn, H = 500m, flaps = 15 deg
   - CAS = 200 kn, H = 3048m, flaps = 0 deg
   - CAS = 250 kn, H = 6100m, flaps = 0 deg
   - CAS = 350 kn, H = 6100m, flaps = 0 deg

6. The nonlinear aircraft simulation runs confirmed that the system satisfied the design requirements for noise free, wind shear, and turbulent conditions.

REFERENCES

1. Terminal Configured Vehicles Program Test Facilities Guide, NASA SP 435, 1980.

2. D. A. Wolverton and C. Stominski, Flight Control Computer Software Description, Computer Science Corporation, TAO Number 18303, June 1982.

3. A. E. Goodwin, NASA 515 Flight Control System Description, RSFS Aircraft, Boeing Commercial Airplane Company, September 1976, NASA Contract 14070.

4. L. G. Malcom and P. L. O'Toole, WWCS Software Description, The Boeing Commercial Airplane Company, D6-42958, November 1976.

5. J. Roskan, Airplane Flight Dynamic and Automatic Flight Controls Pt. II, University of Kansas, 1979.

6. ACSL—Advanced Continuous Simulation Language, User Guide/Reference Manual Mitchel and Gauthier Associates 2nd Edition 1975.

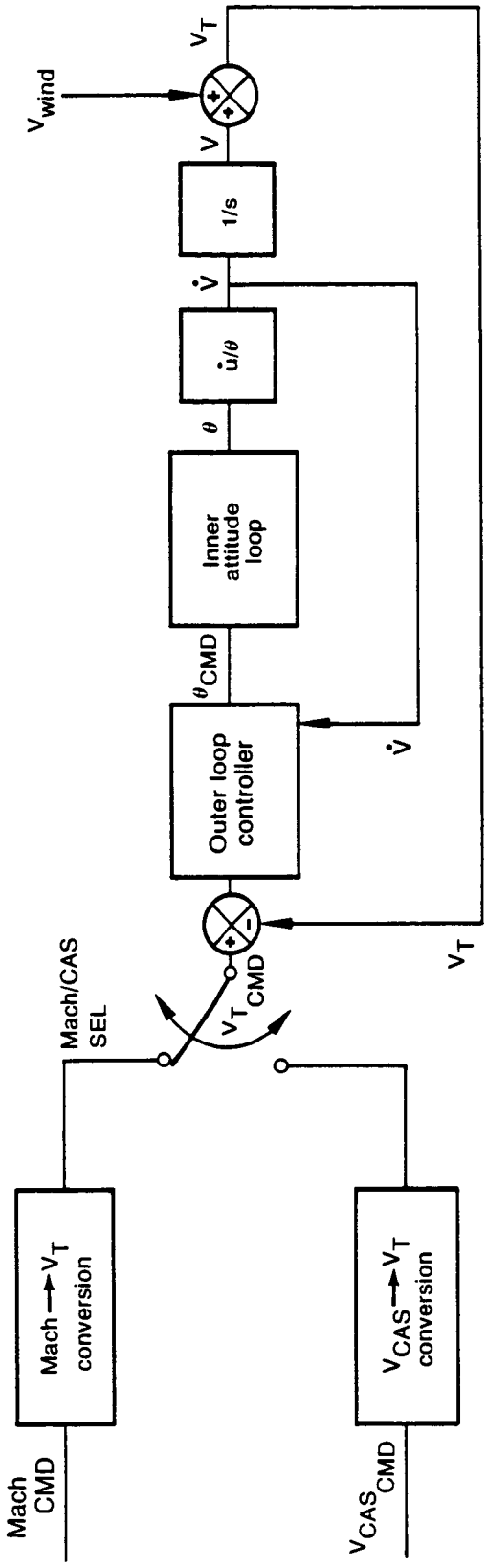

Figure 1. Simplified Block Diagram of Control Law

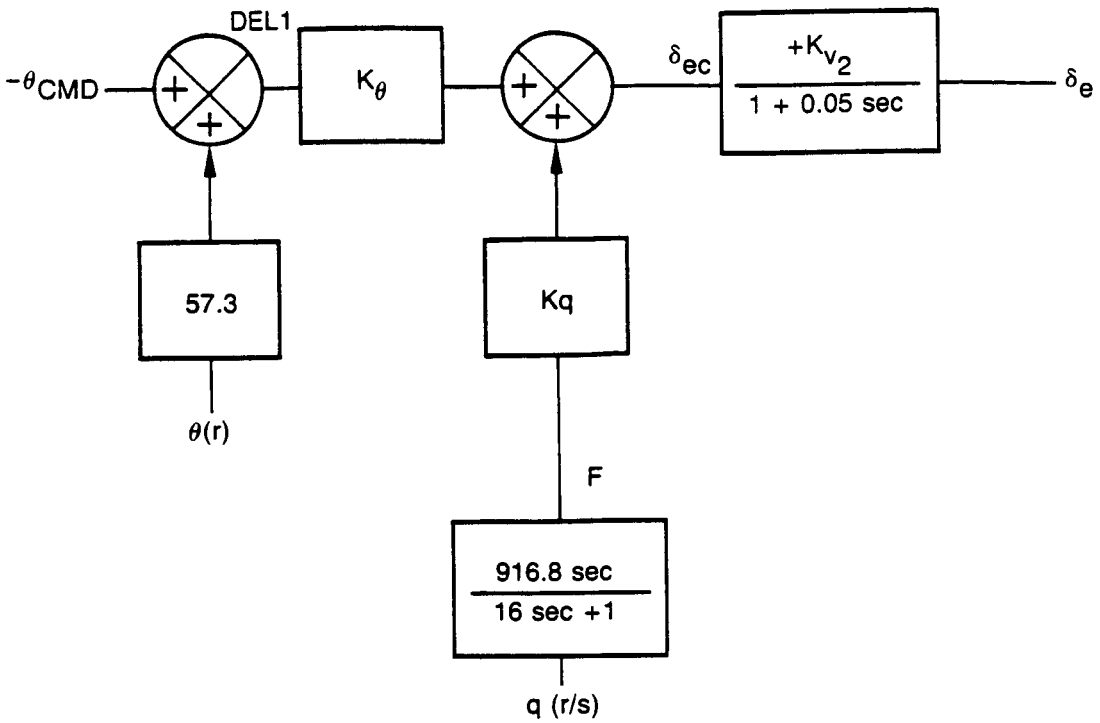

Figure 2. Inner Loop Autopilot Loop

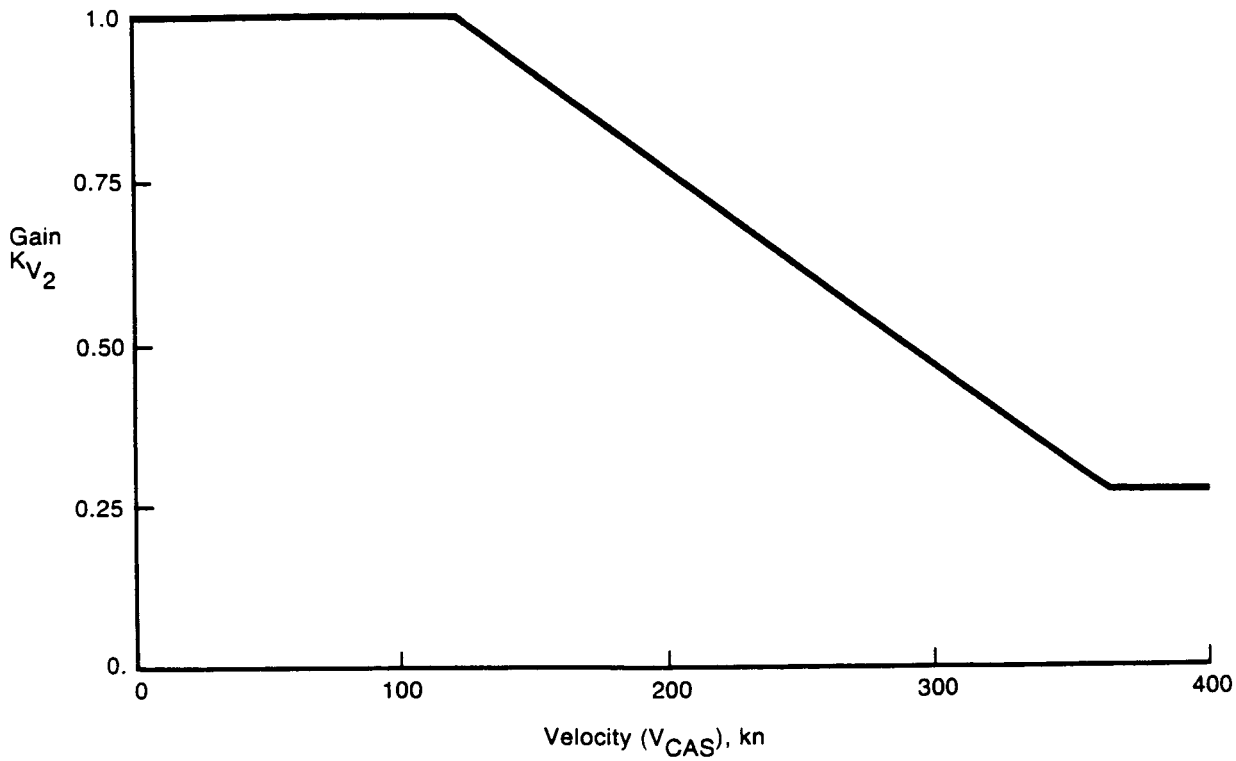

Figure 3. Gain Scheduling for K_{V_2}

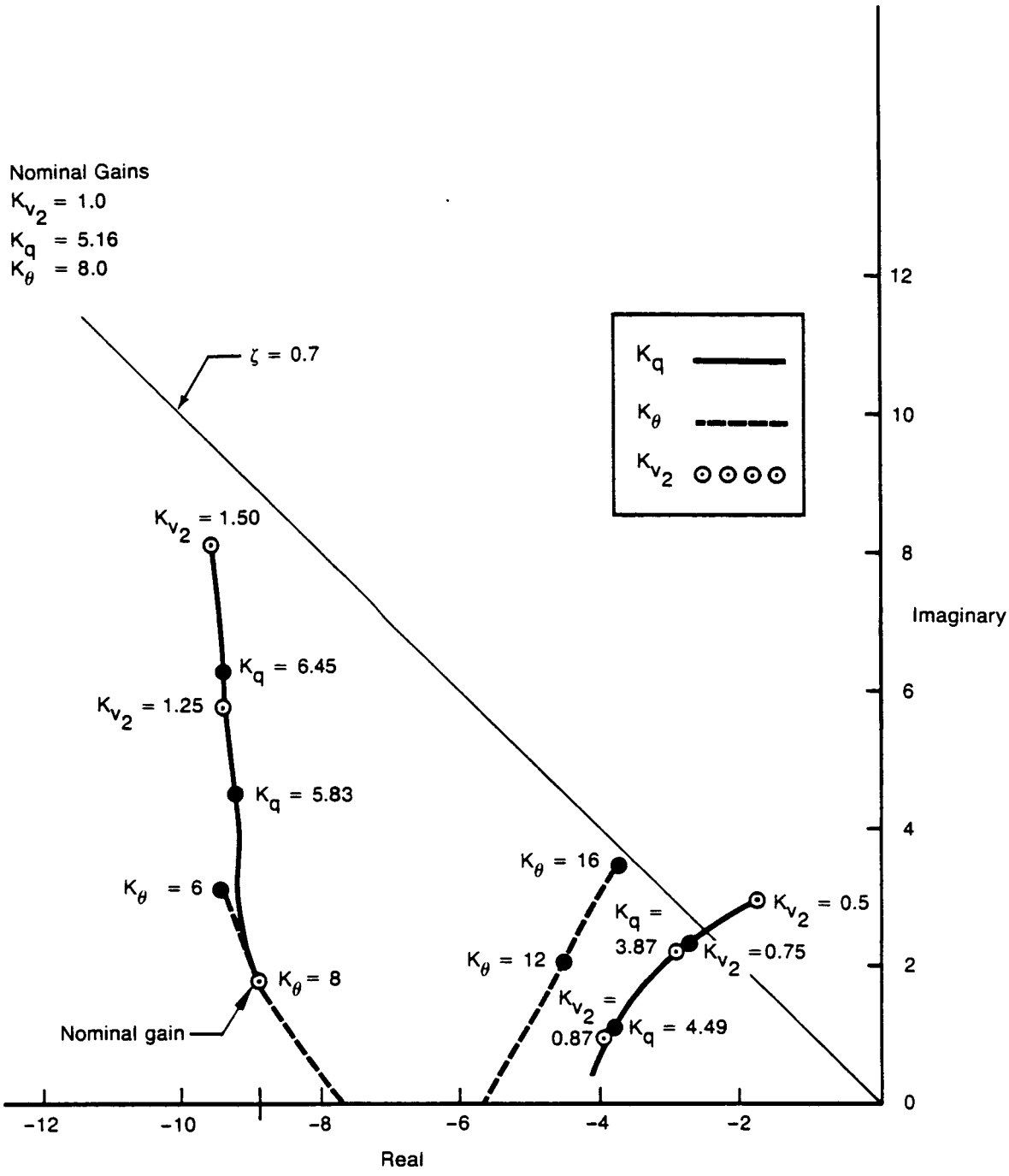

Figure 4. Root Locus for Dominant Complex Poles Inner Loop, Low-Speed Case (θ, $\dot{\theta}$ Feedback Only)

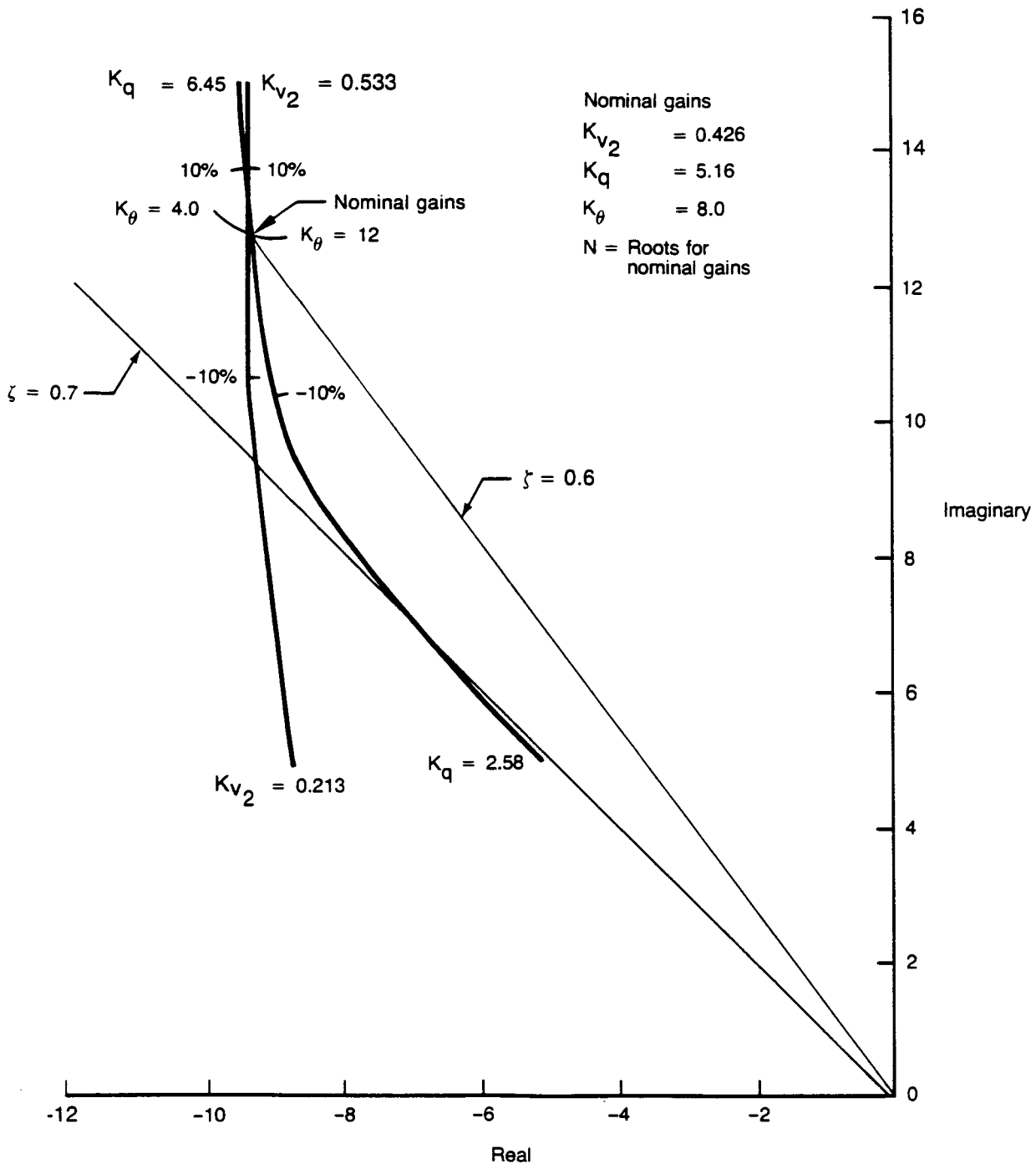

Figure 5. Root Locus of Dominant Complex Poles Inner Loop, High-Speed Case (θ, $\dot{\theta}$ Feedback Only)

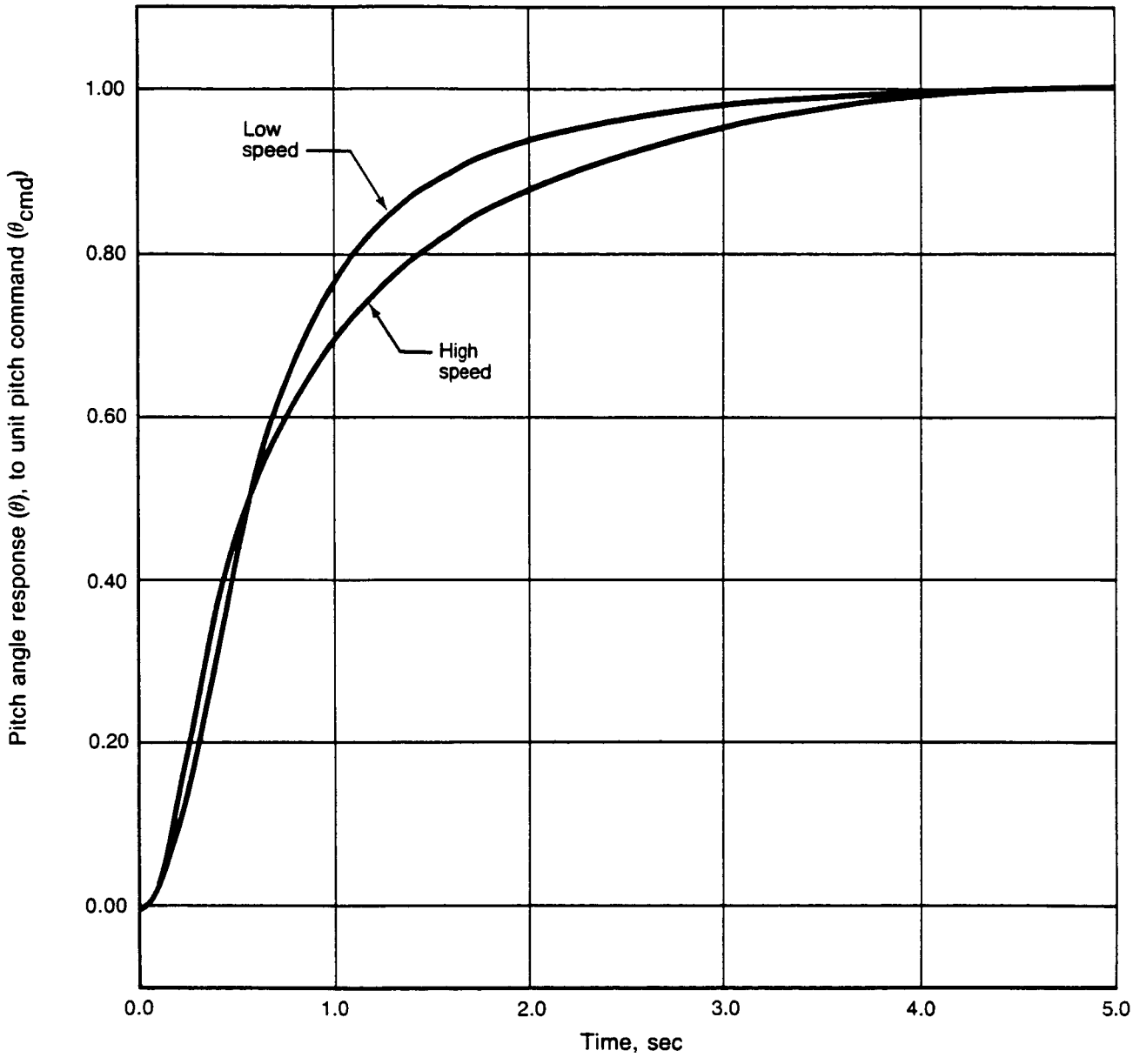

Figure 6. Transient Response to Unit Step (High and Low Speed)

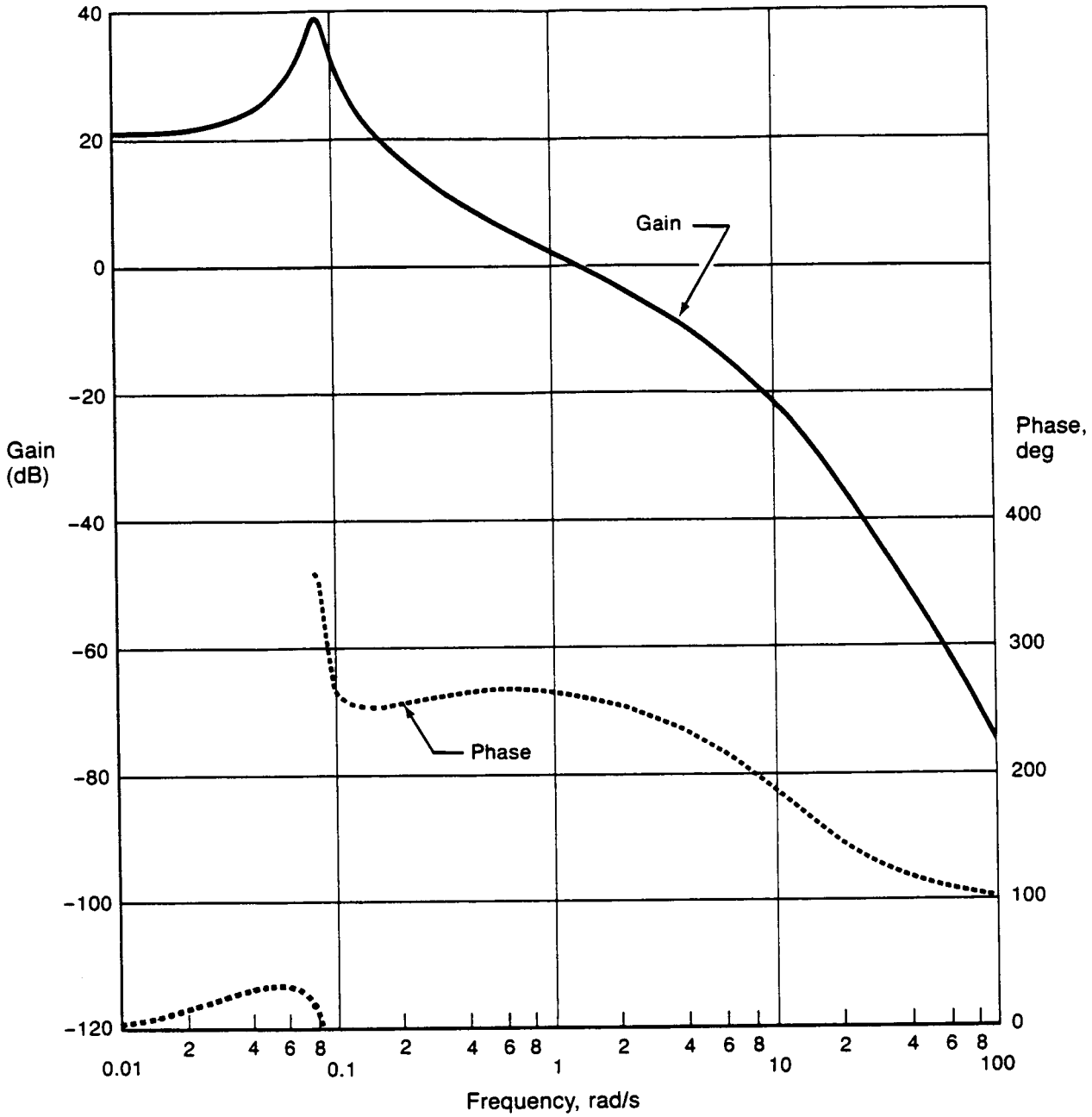

Figure 7. Low-Speed, Open Loop Frequency Response

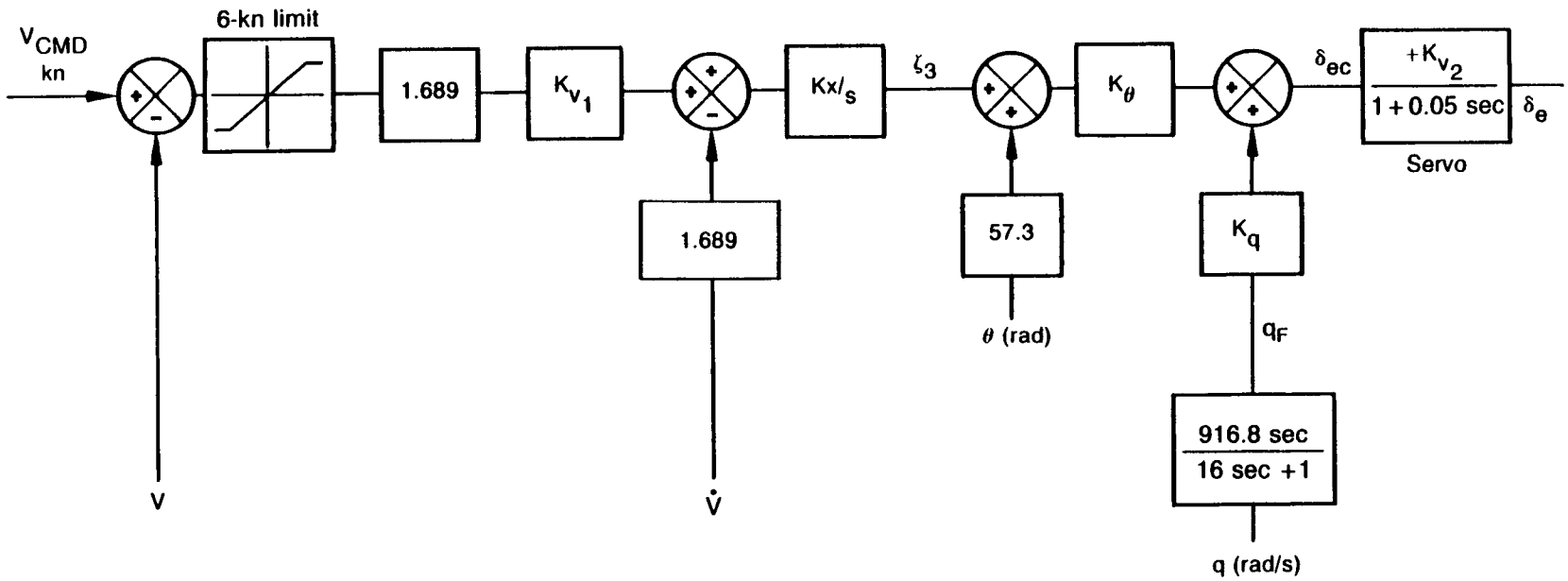

Figure 8. Mach/CAS Control Law

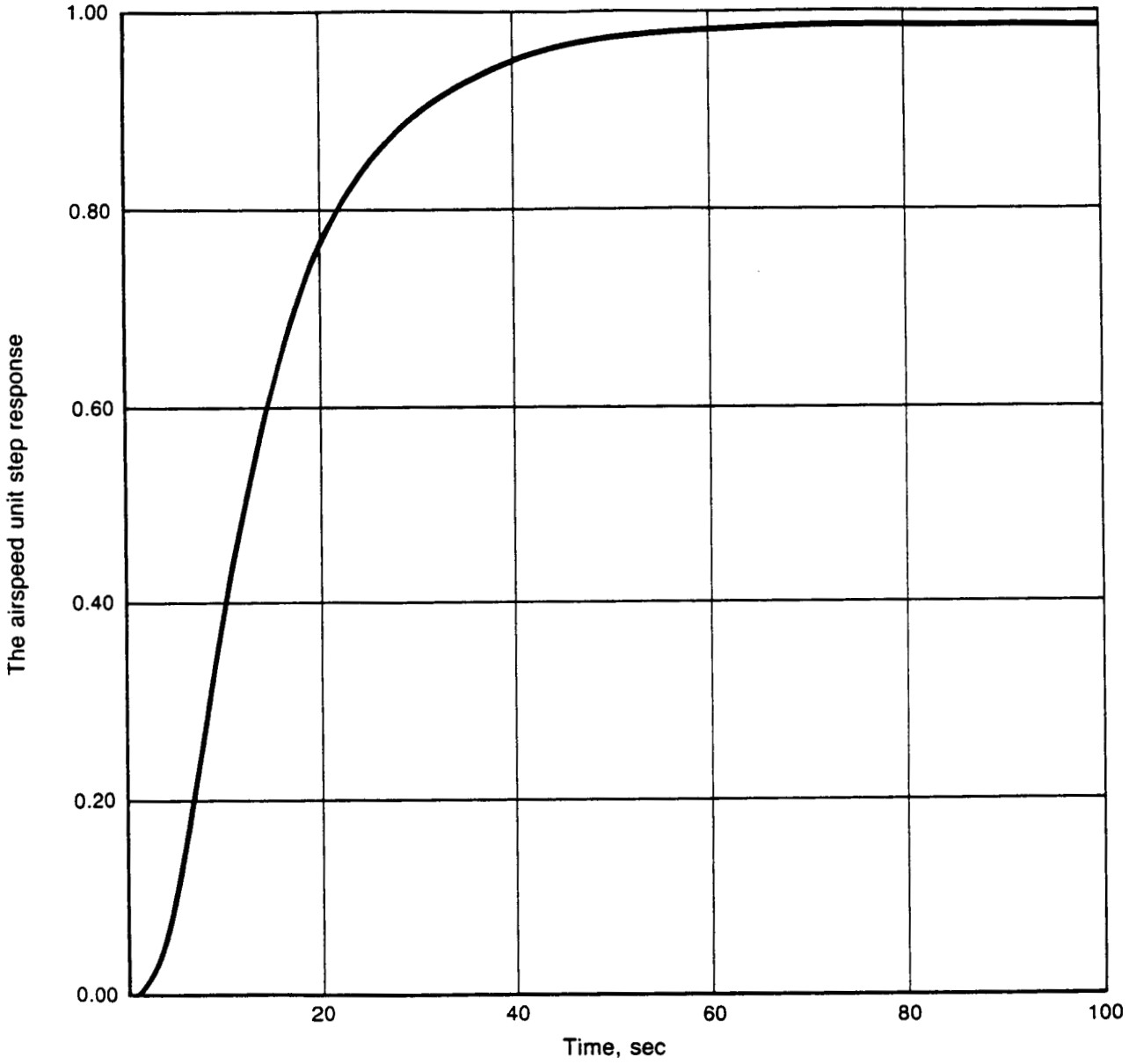

Figure 9. Response of Velocity Hold Loop to Unit Step (Low-Speed Case)

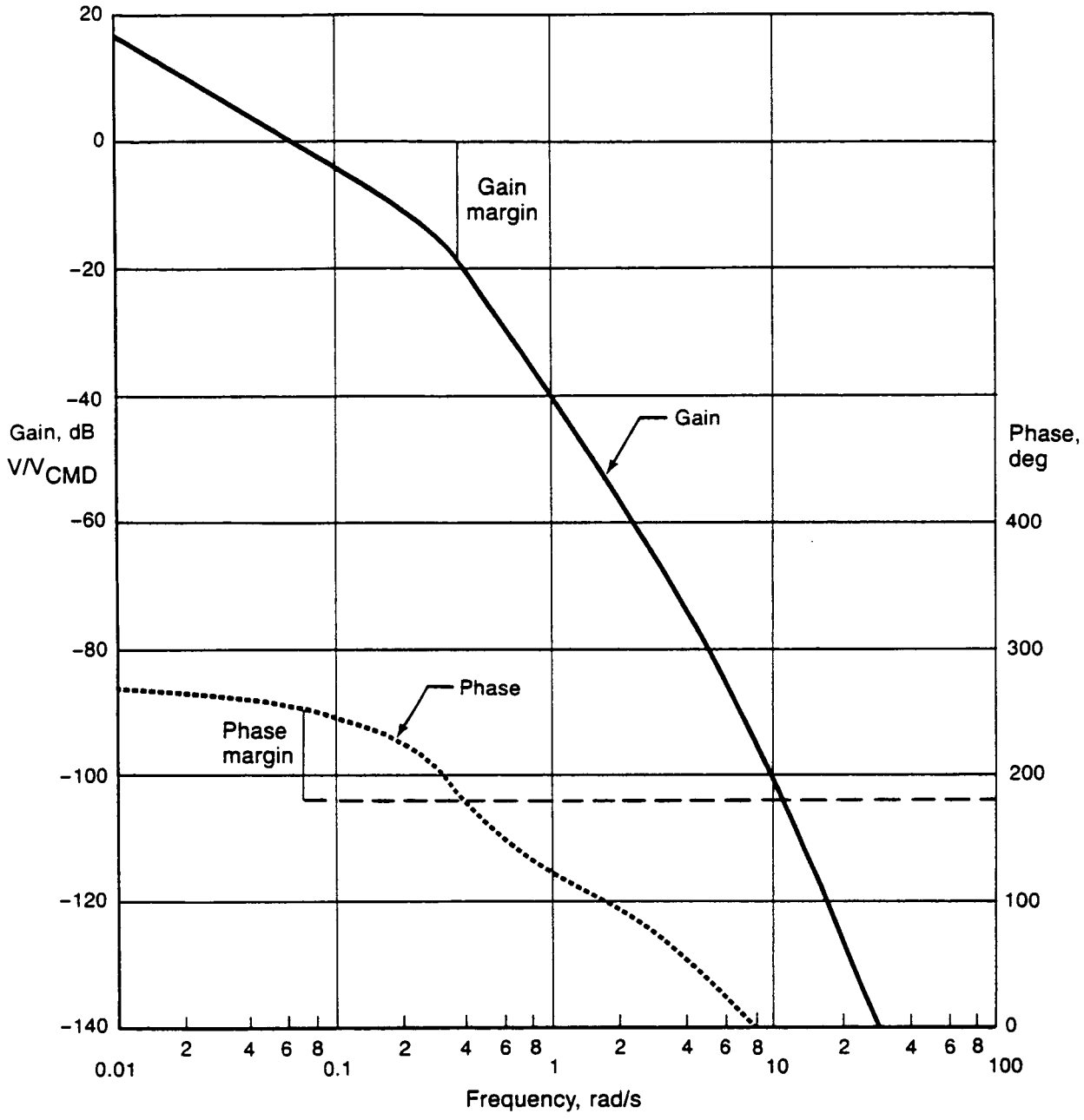

Figure 10. Velocity Hold Loop Frequency Response (Low Speed), Open Loop

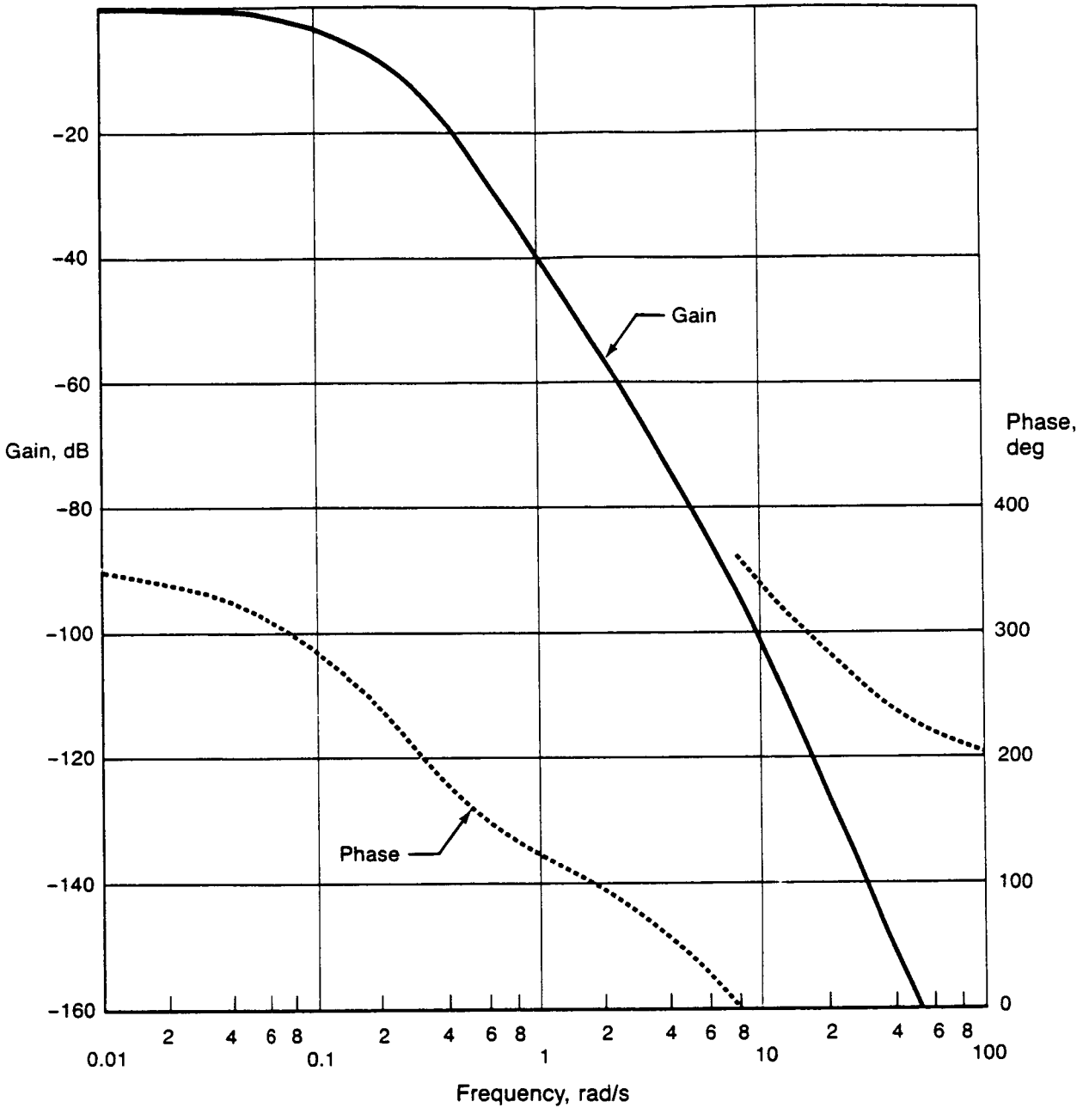

Figure 11. Velocity Hold Loop Frequency Response (Low Speed), Closed Loop

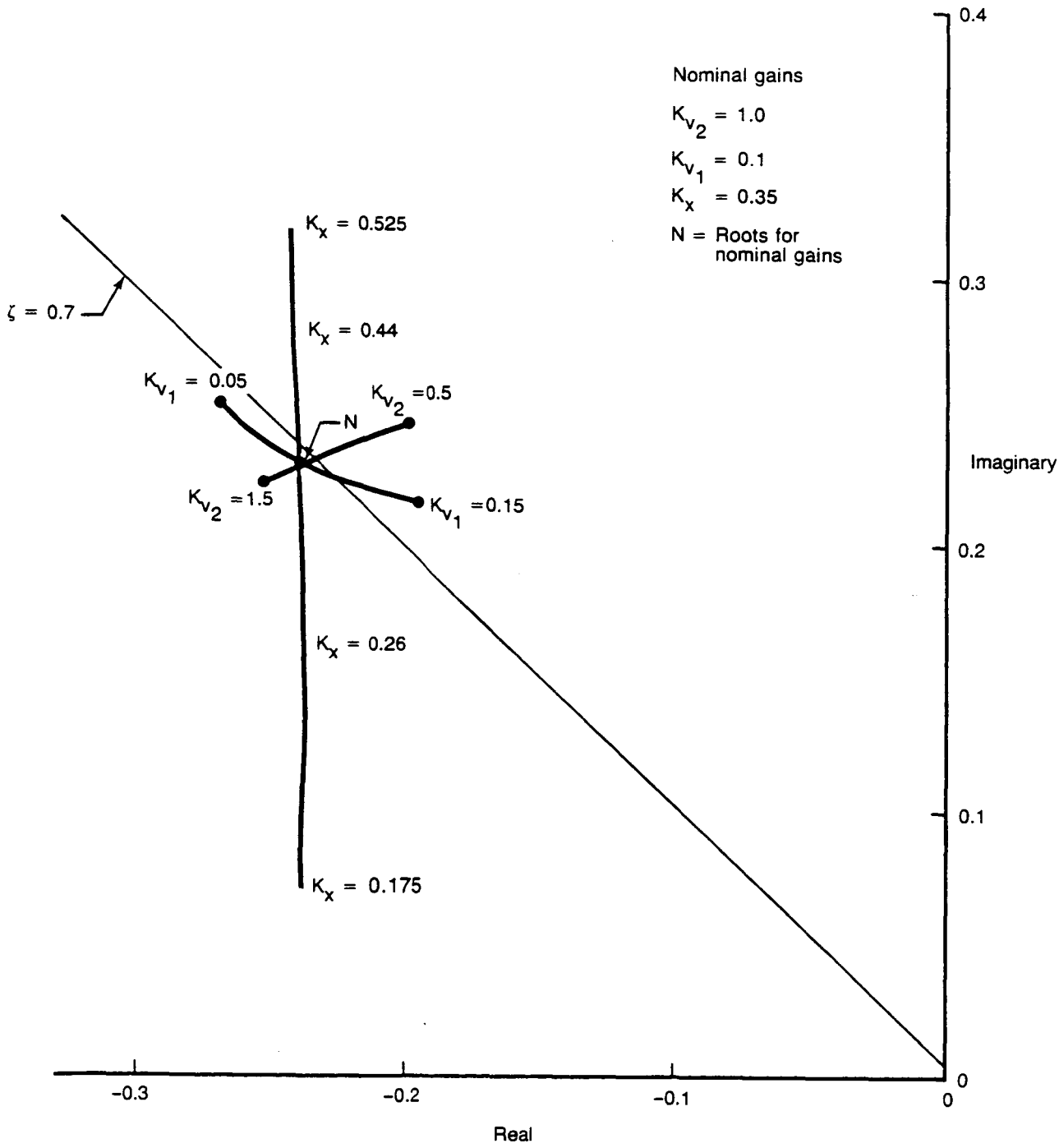

Figure 12. Root Locus for Dominant Complex Poles (Outer Loop, Low-Speed Case)

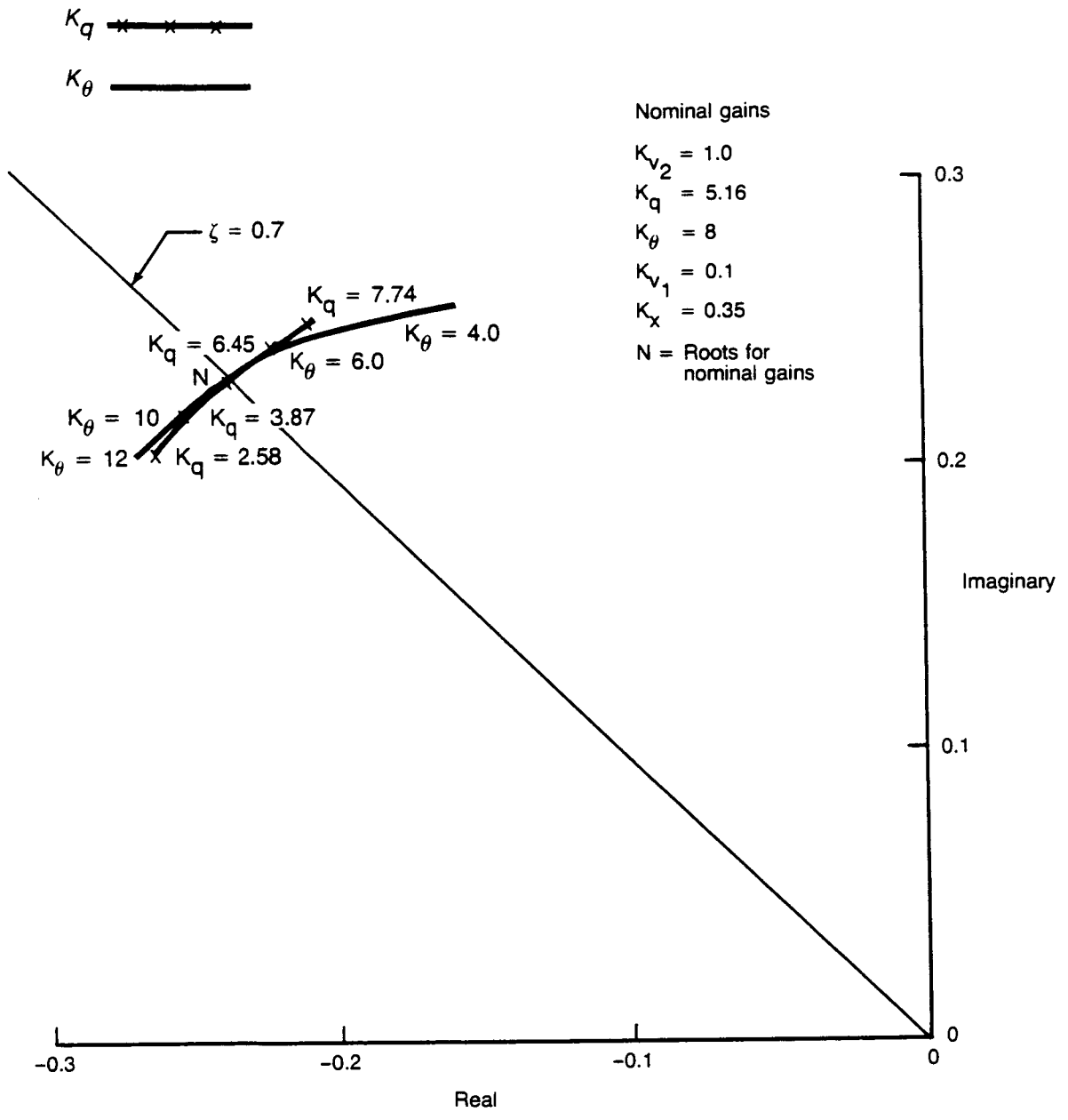

Figure 13. Root Locus for Dominant Complex Poles (Outer Loop, Low-Speed Case)

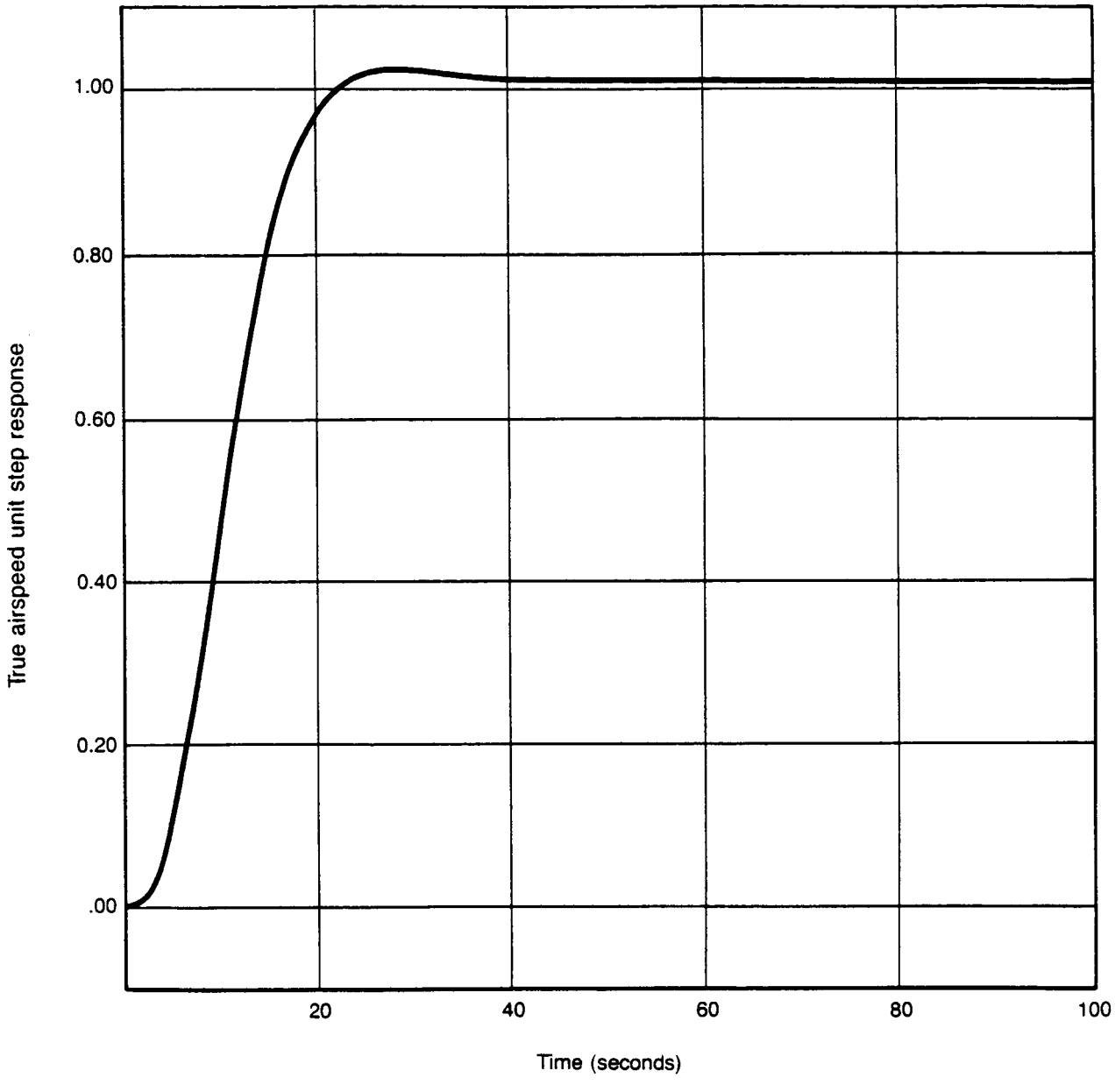

Figure 14. Response of Velocity Hold Loop to Unit Step (High-Speed Case)

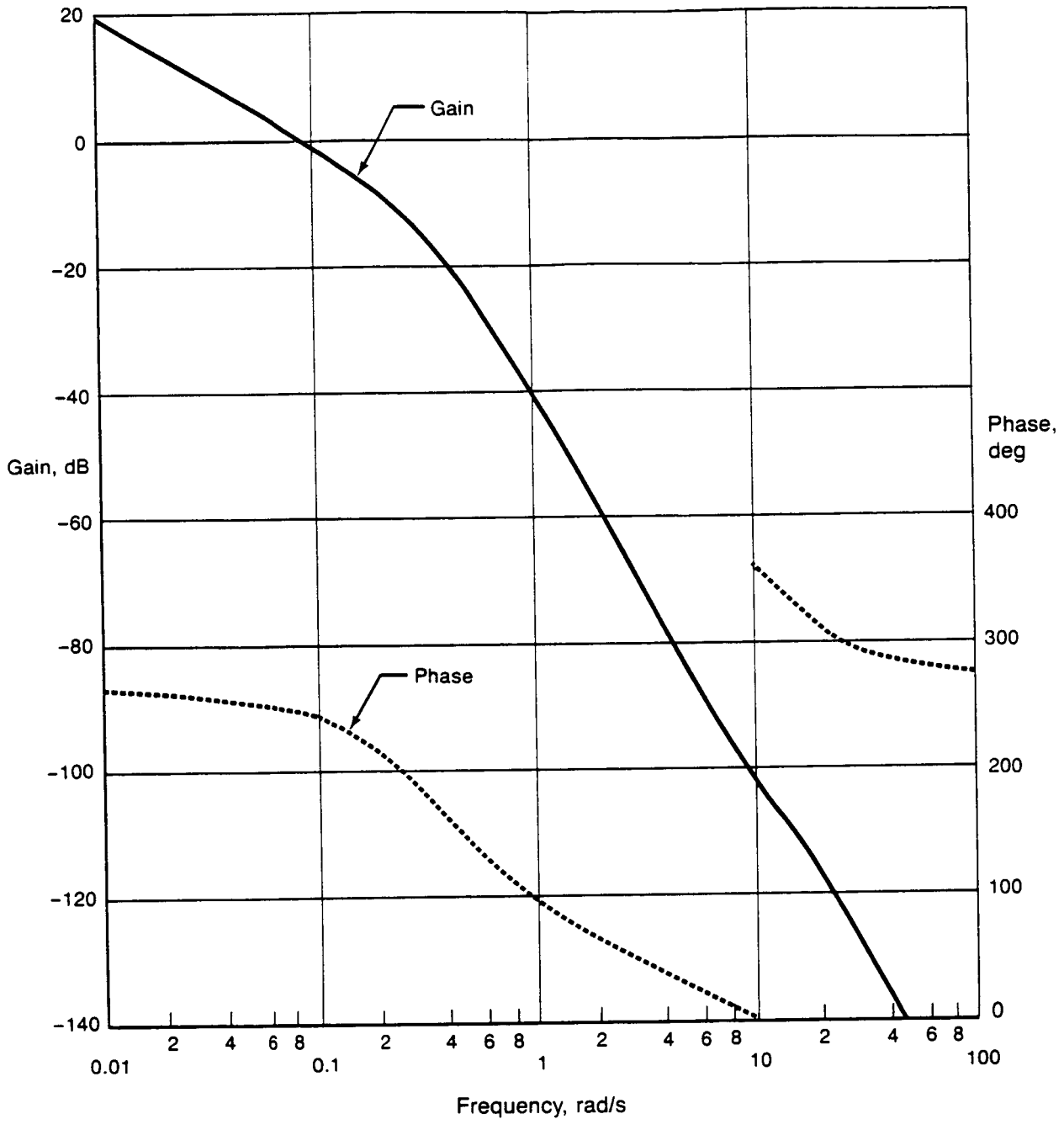

Frequency response open loop VTAS/VCMD

Figure 15. Open Loop Frequency Response (High-Speed Case)

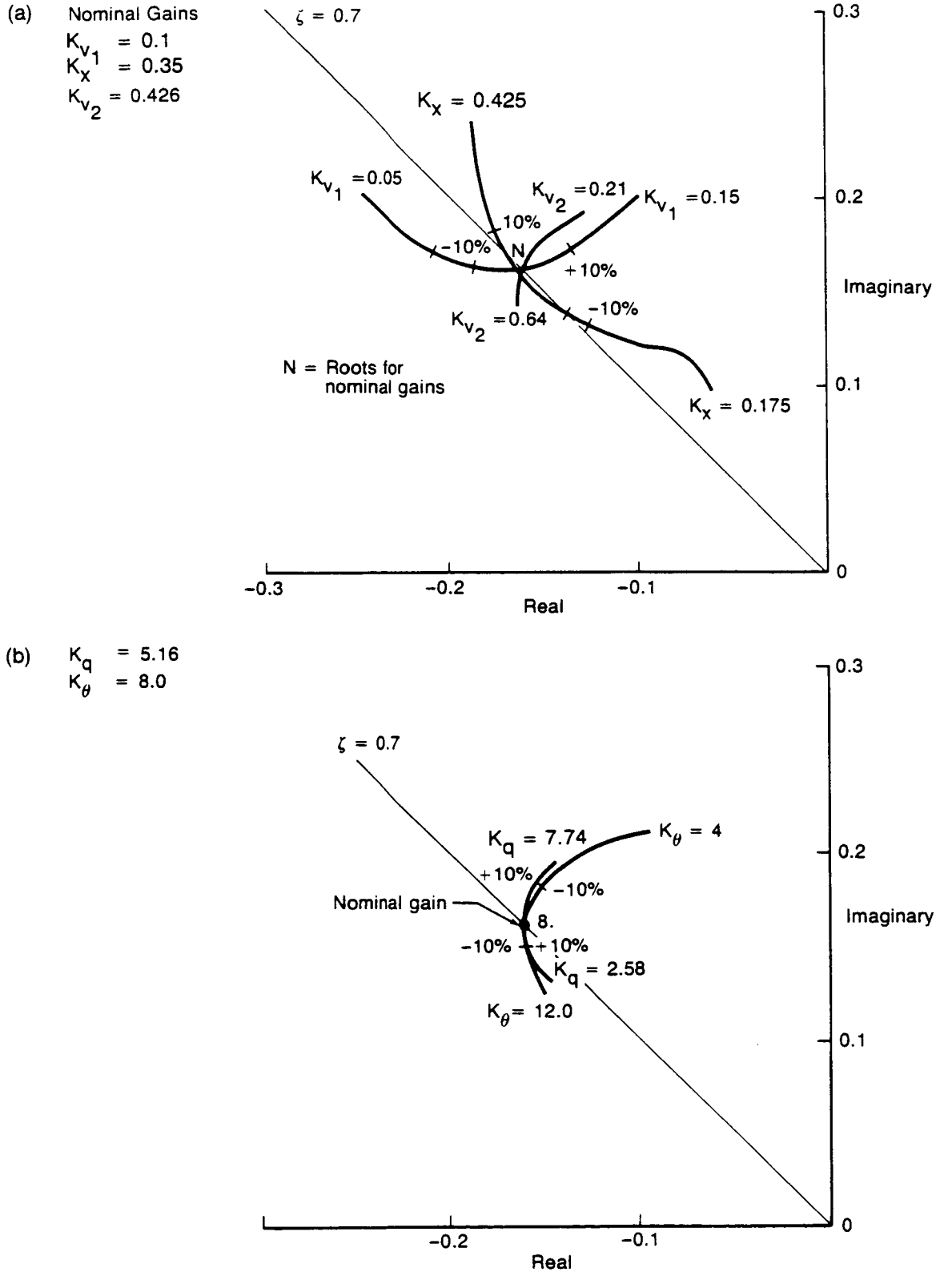

Figure 16. Root Locus for Dominant Complex Roots (High-Speed Case)

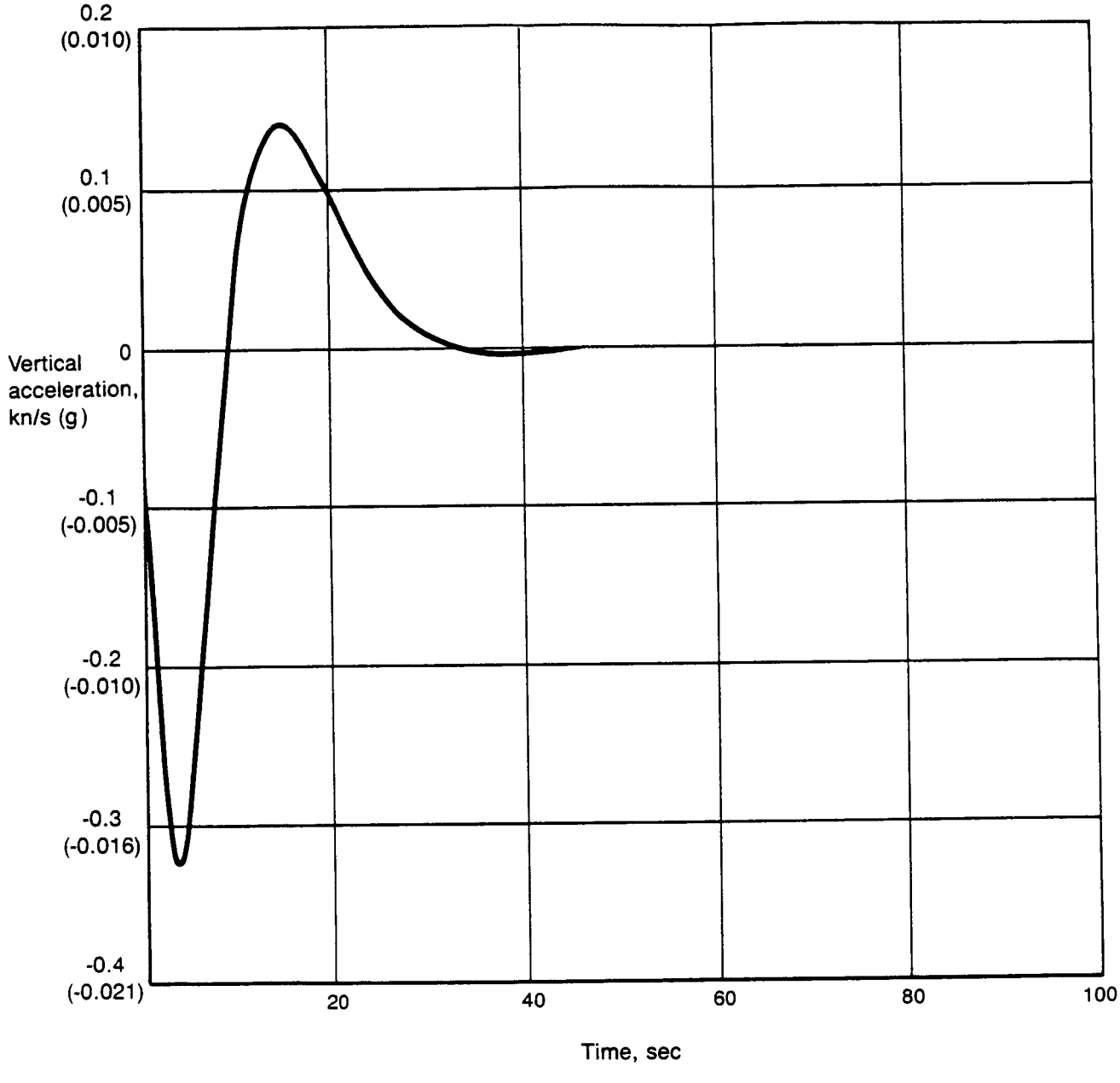

Figure 17. Vertical Acceleration for 1-kn Step Input (High Speed)

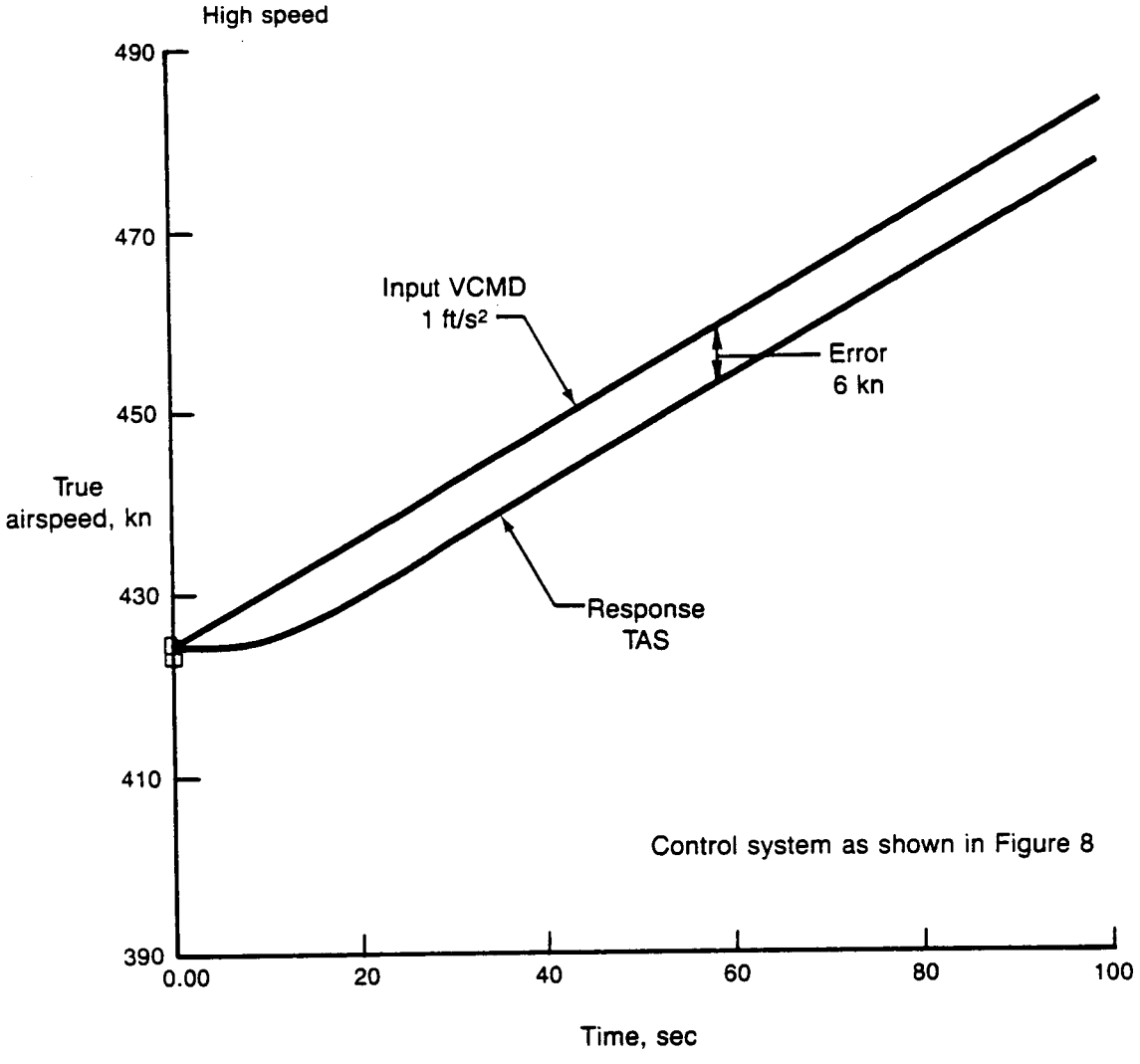

Figure 18. Response to Ramp Input (High Speed)

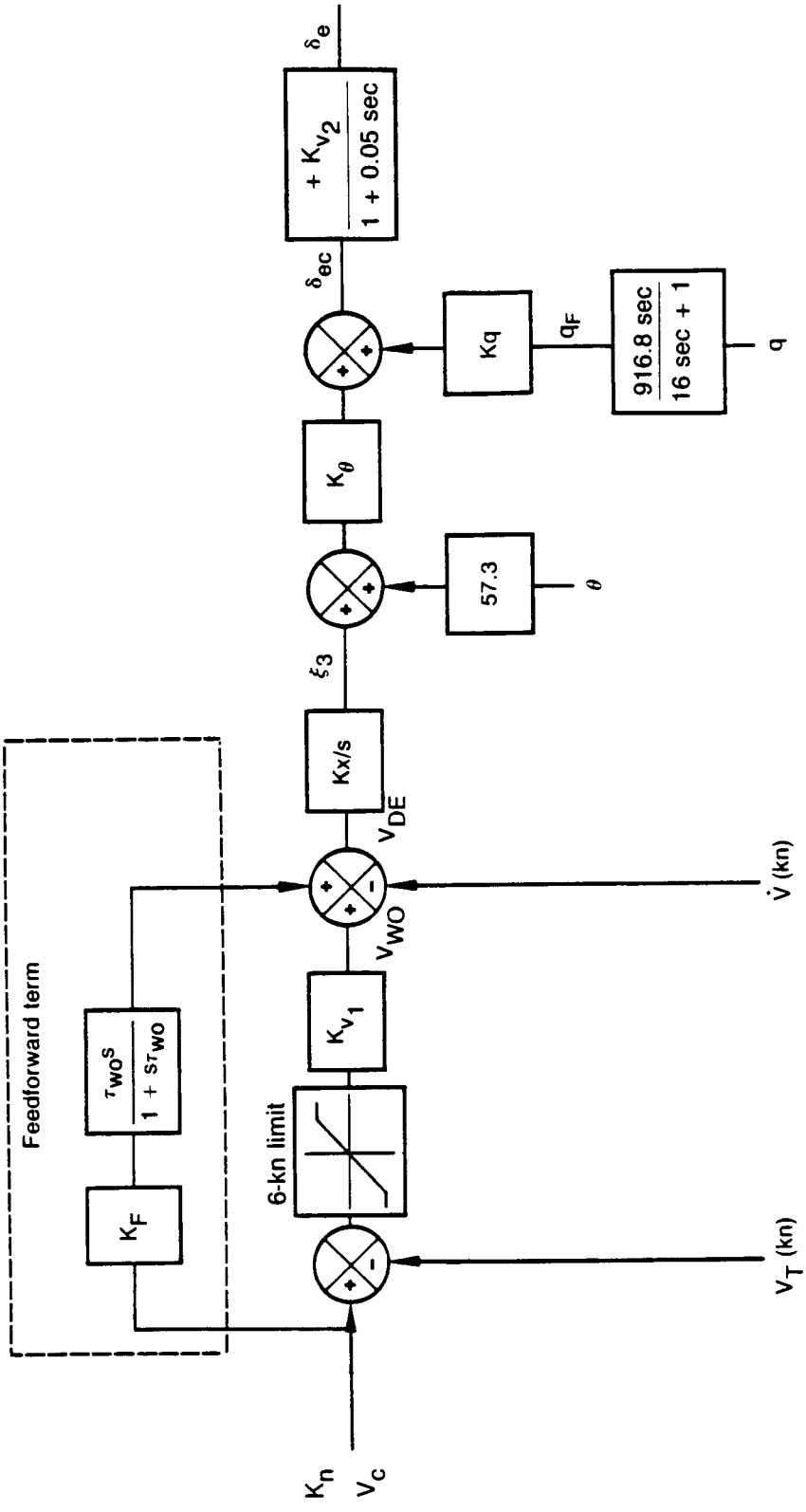

Figure 19. Mach/CAS Control Law With Derivative Feed Forward Team

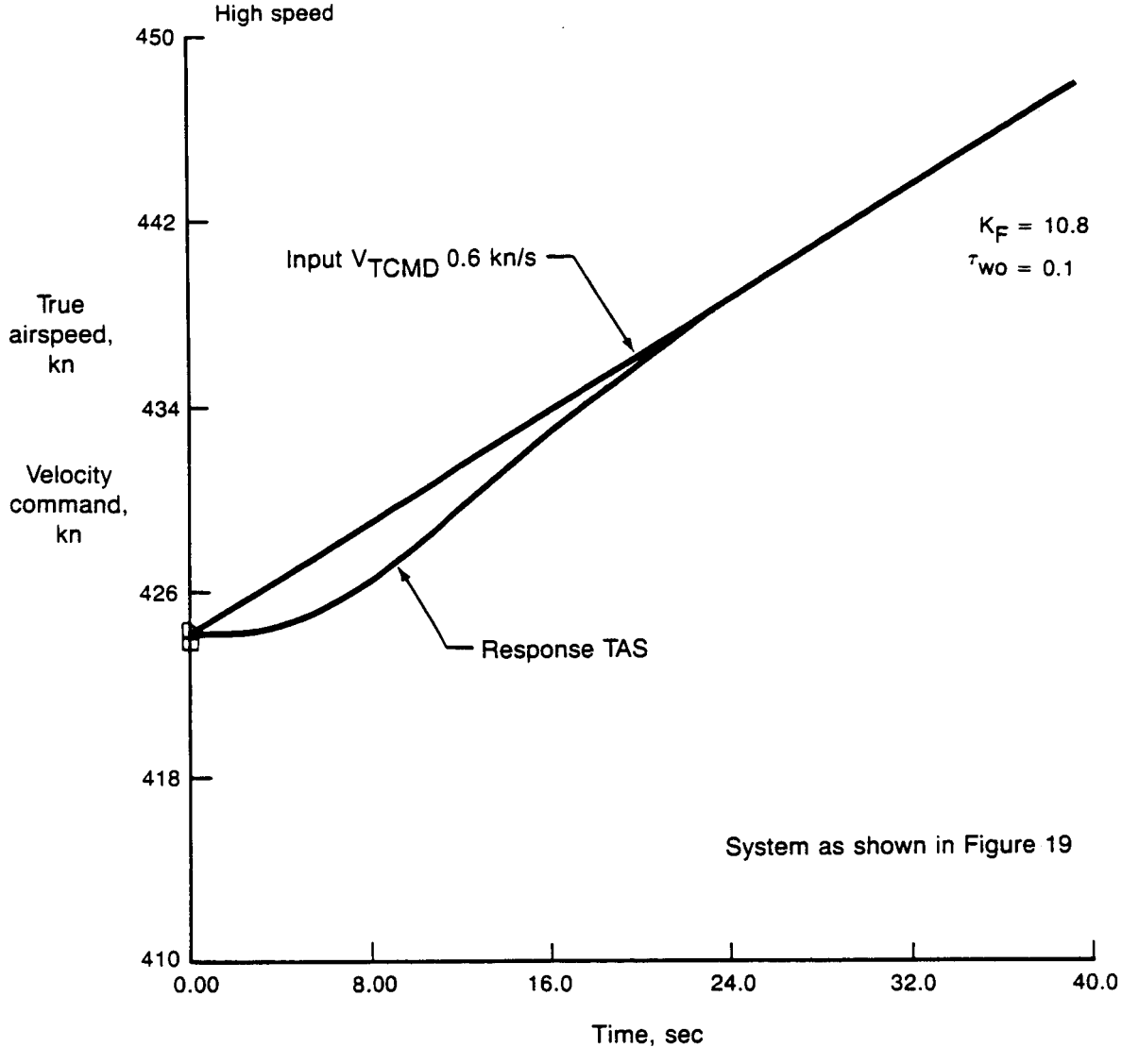

Figure 20. Derivative Feedforward Term: Ramp Response

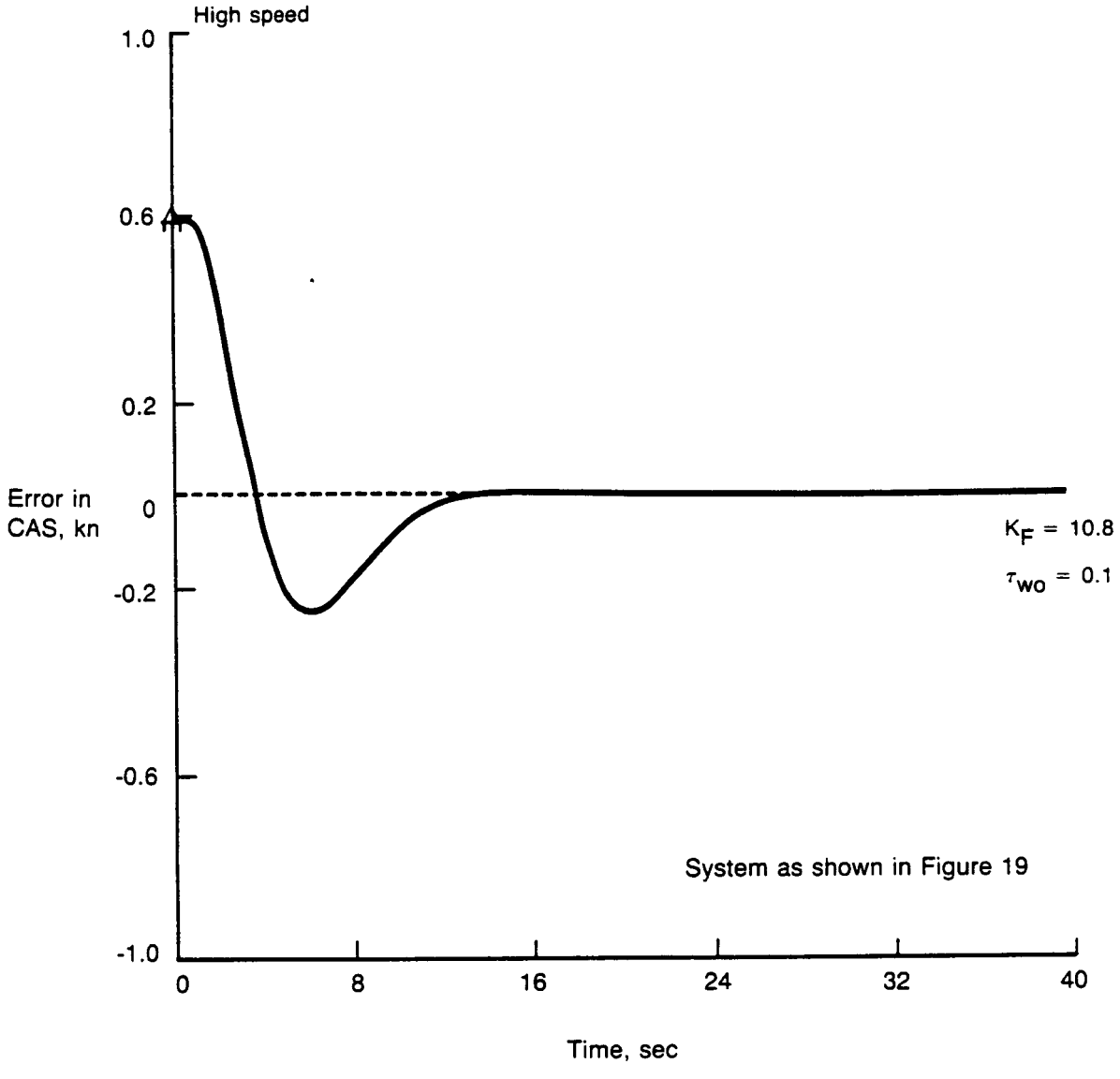

Figure 21. Derivative Feedforward Term: Step Response

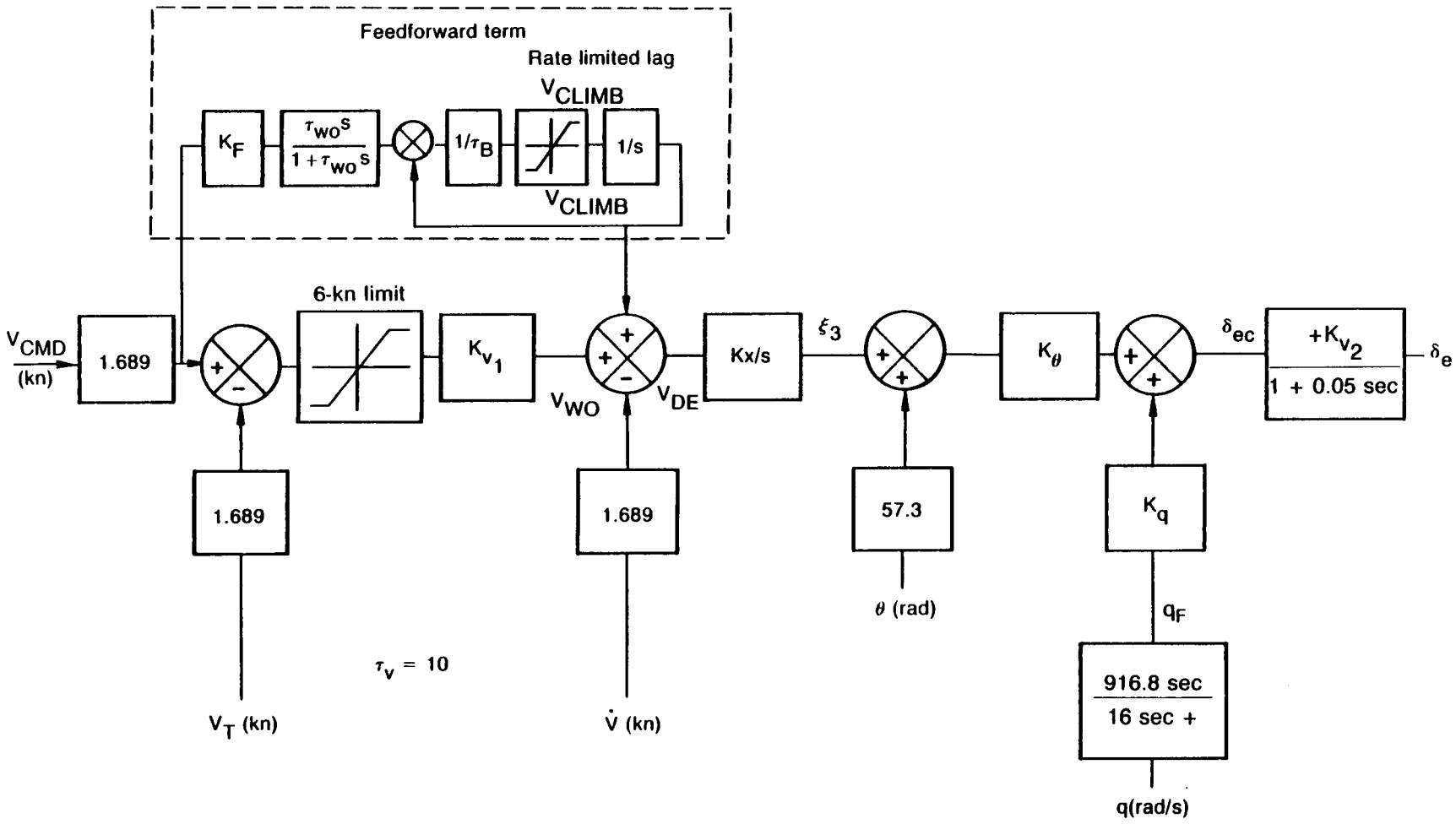

Figure 22. Mach/CAS Control Law With Feedforward Term With Rate Limited Lag

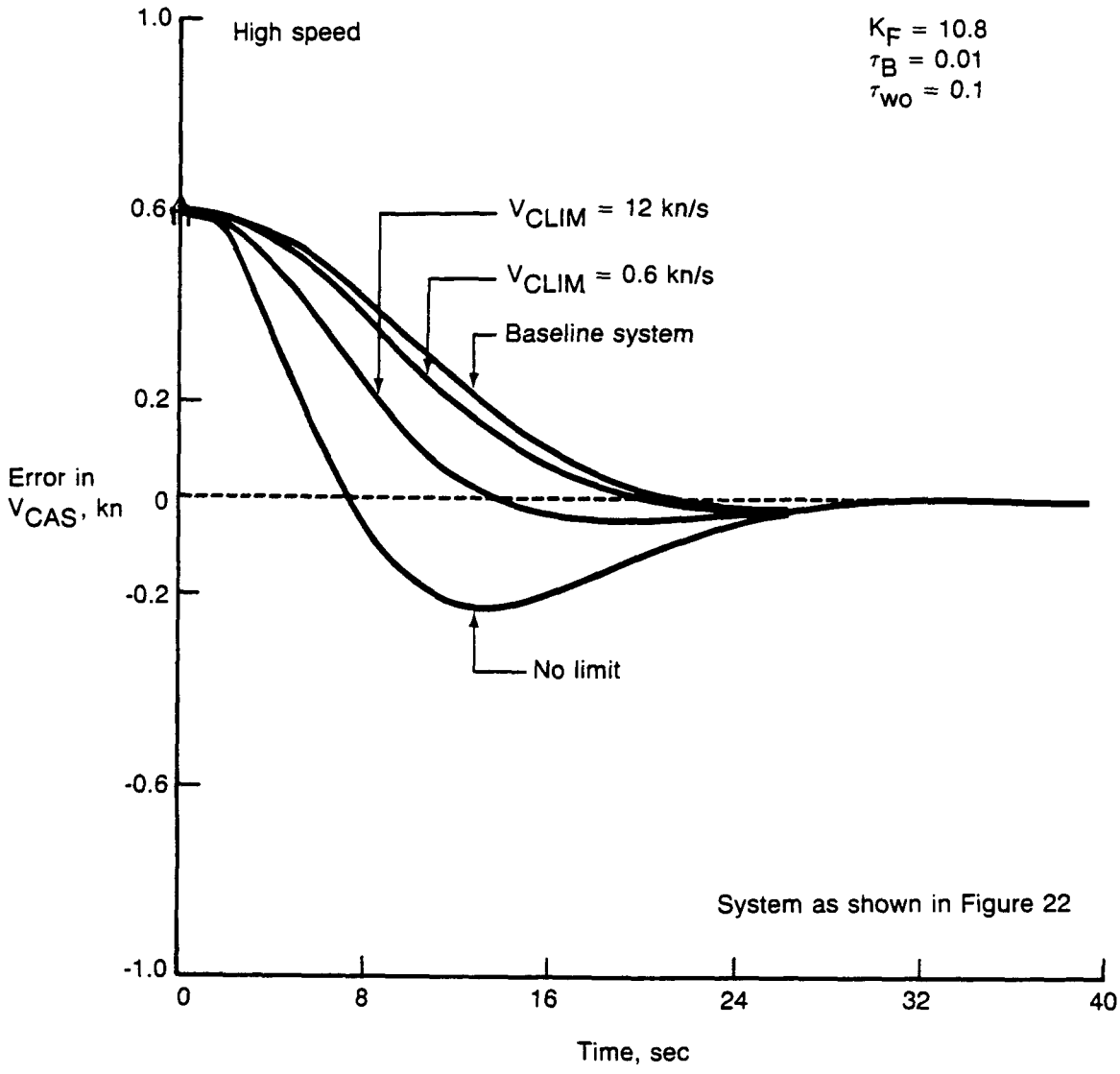

Figure 23. Step Response for Variation in Rate Limit (V_{CLIM})

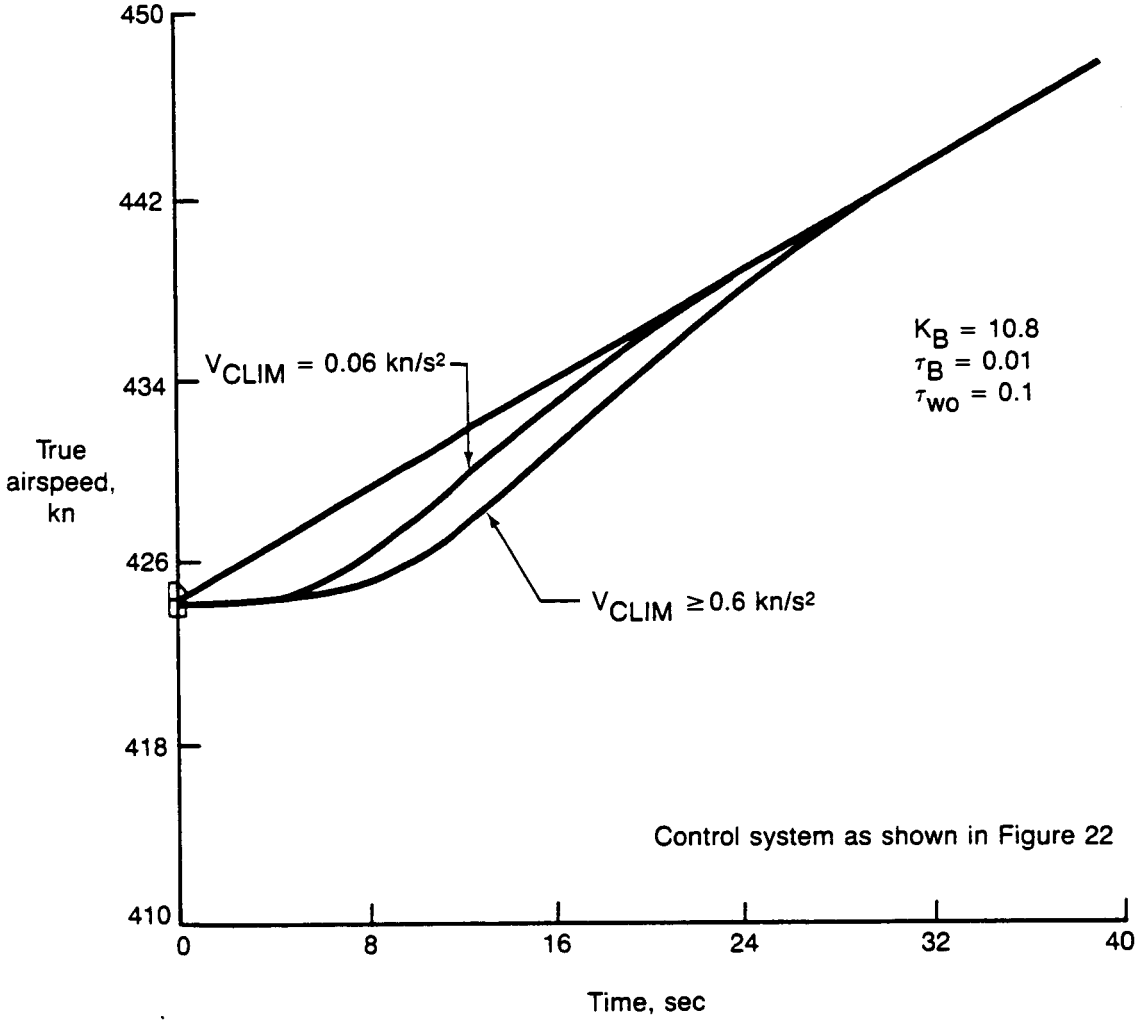

Figure 24. Ramp Response for Variation in Rate Limit (V_{CLIM})

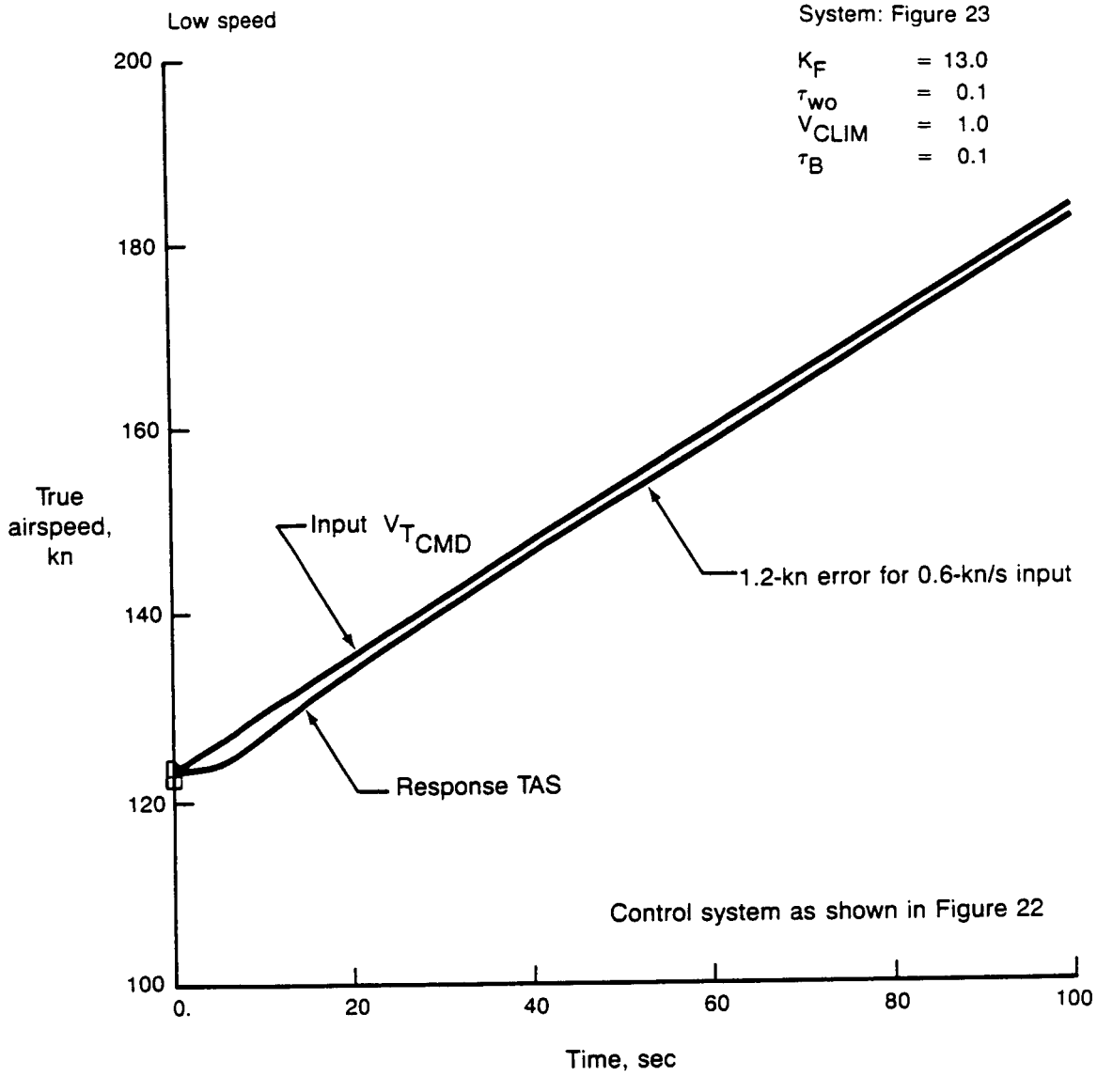

Figure 25. Final Low-Speed Response

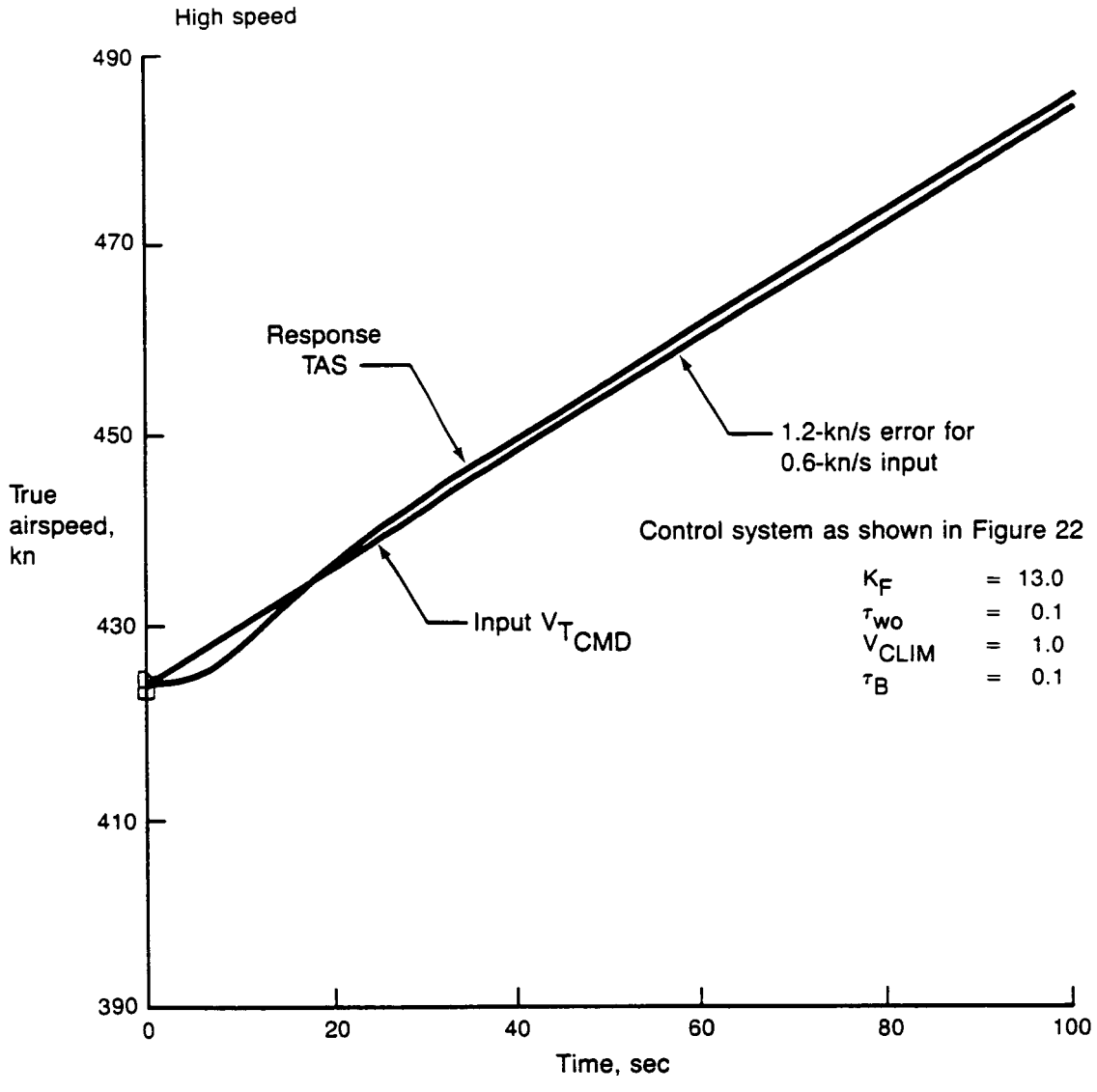

Figure 26. Final High-Speed Response

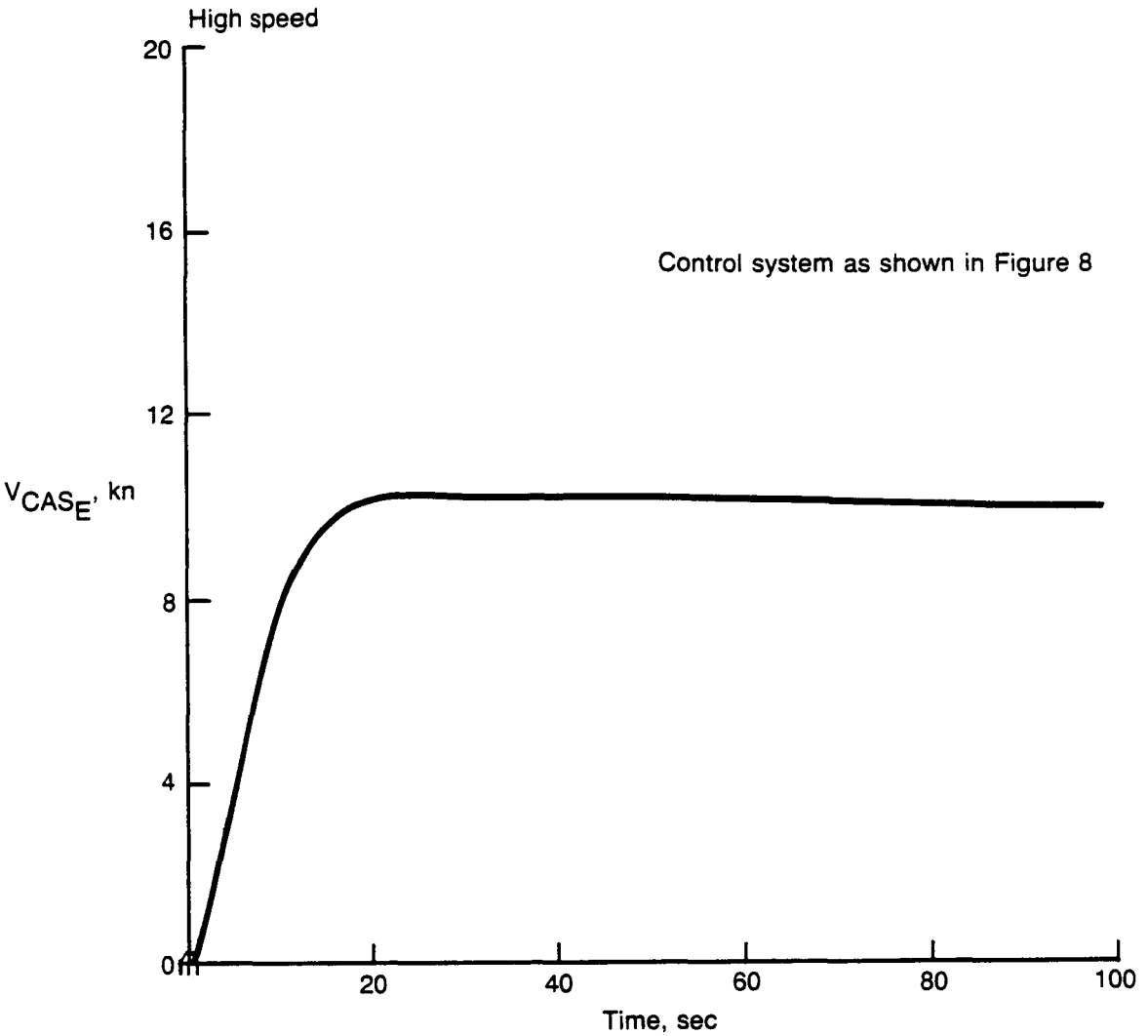

Figure 27. Steady State Calibrated Airspeed Error Due to Wind Shear of 1 kn/s

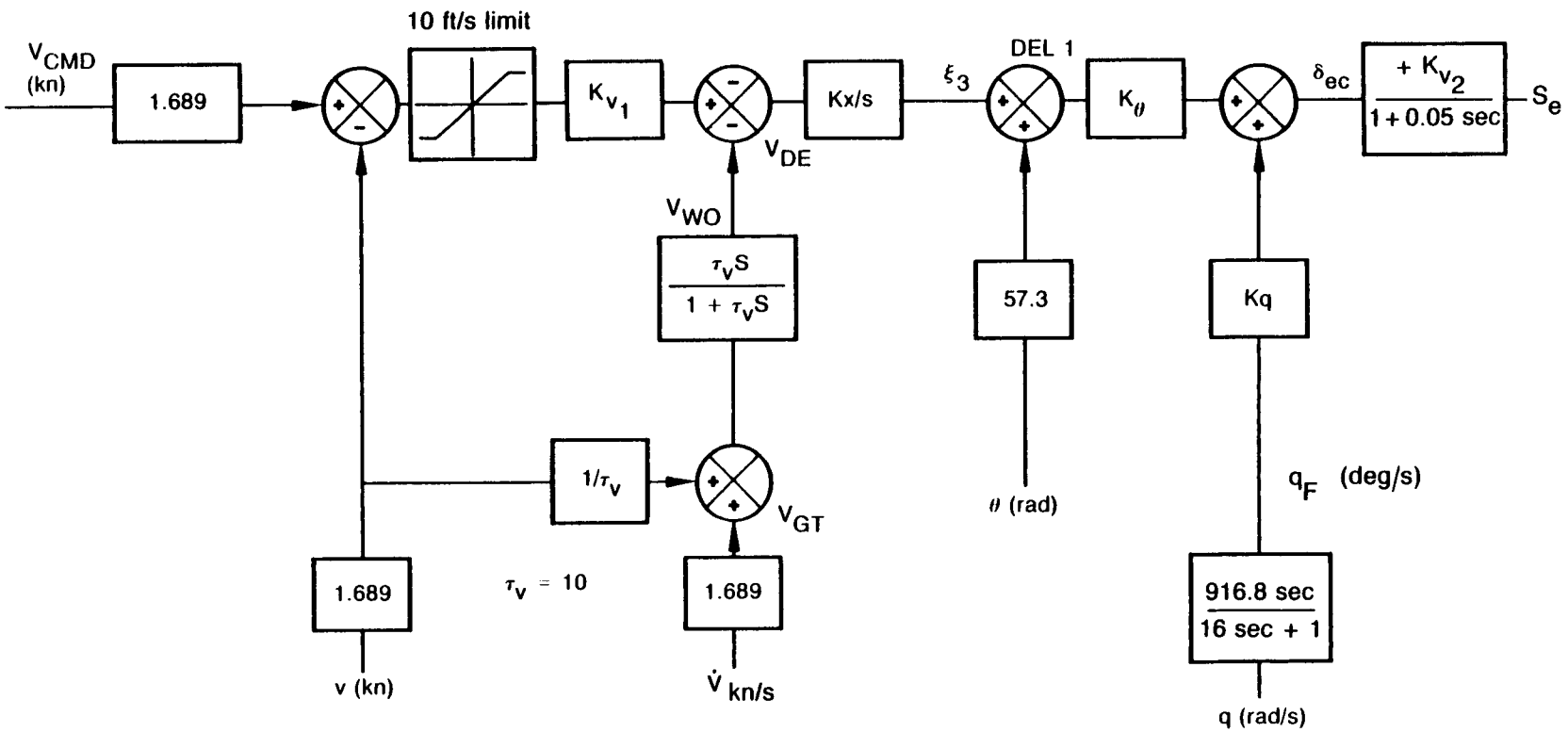

Figure 28. Mach/CAS Control Law With Complementary Filter in Velocity Feedback Loop

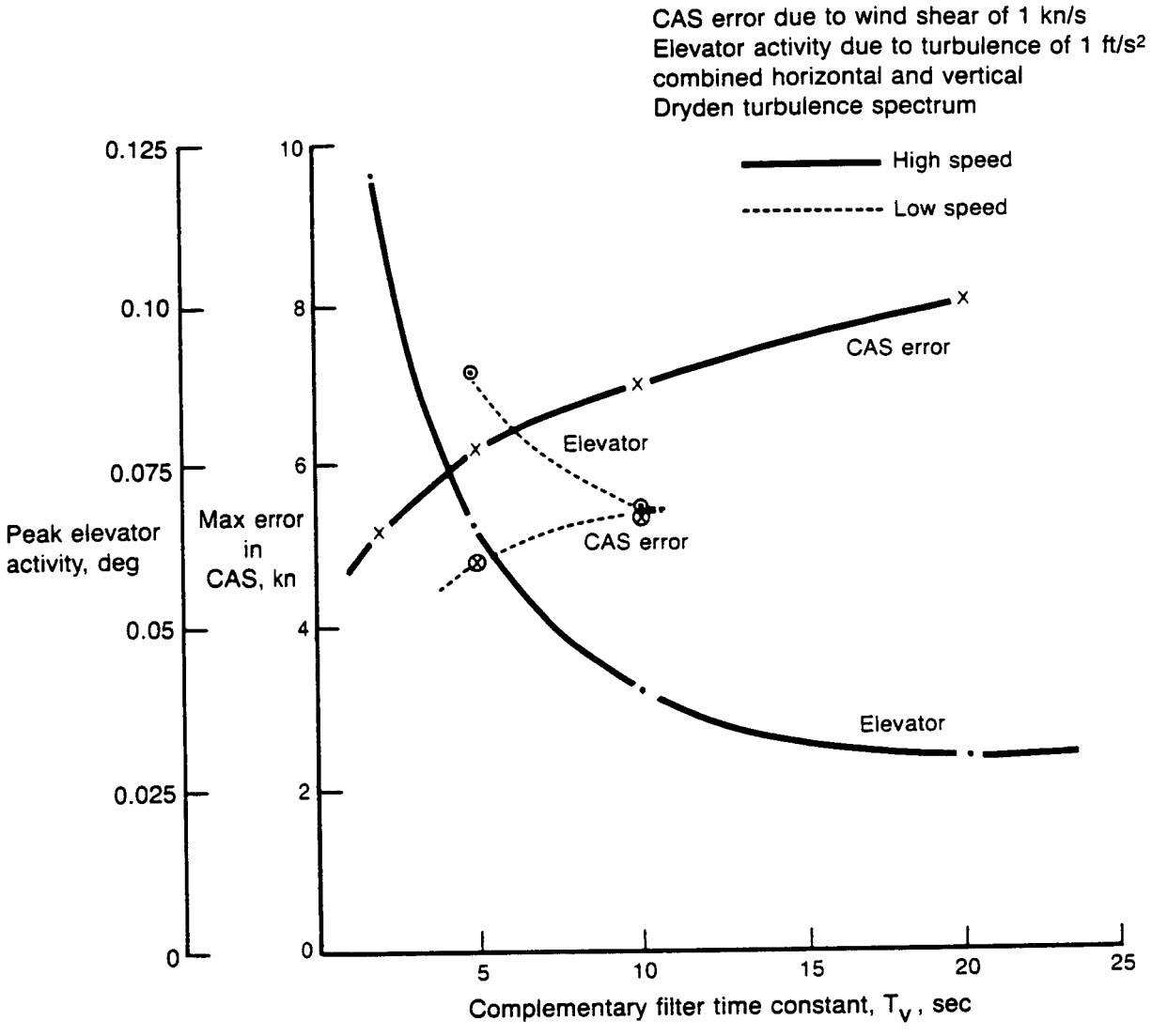

Figure 29. Elevator Activity and CAS Error Versus Complementary Filter Time Constant for Wind Shear of 1 kn/s

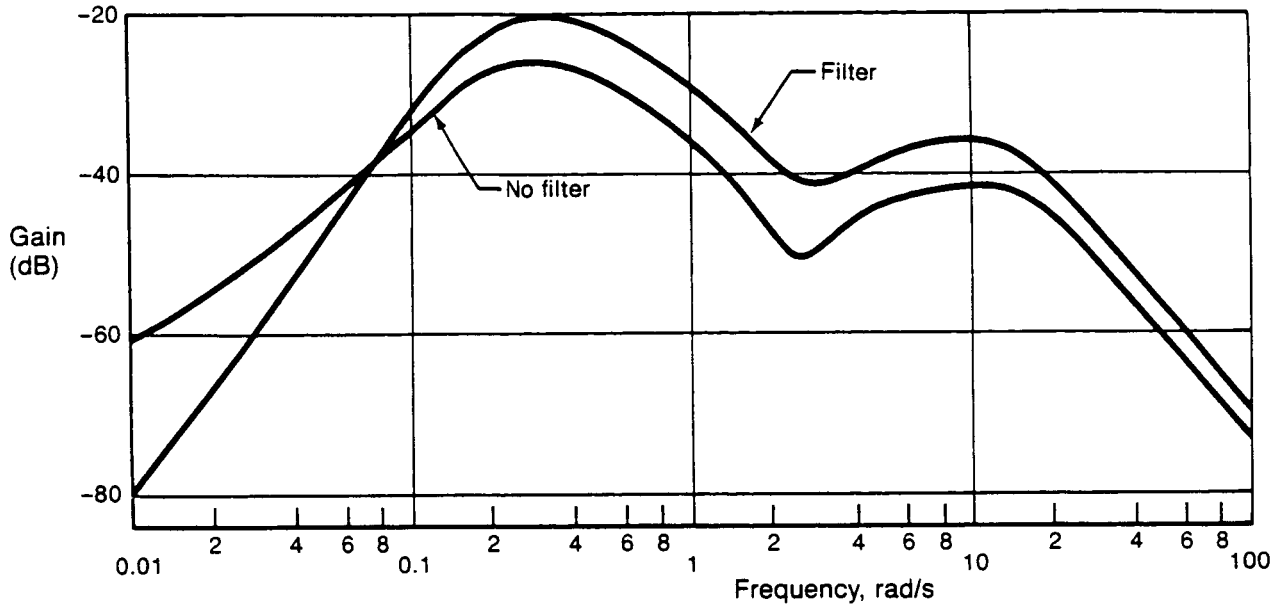

Figure 30. Frequency Response of Elevator $\delta_{e/u}$ (deg) (With and Without Complementary Filter) (High Speed)

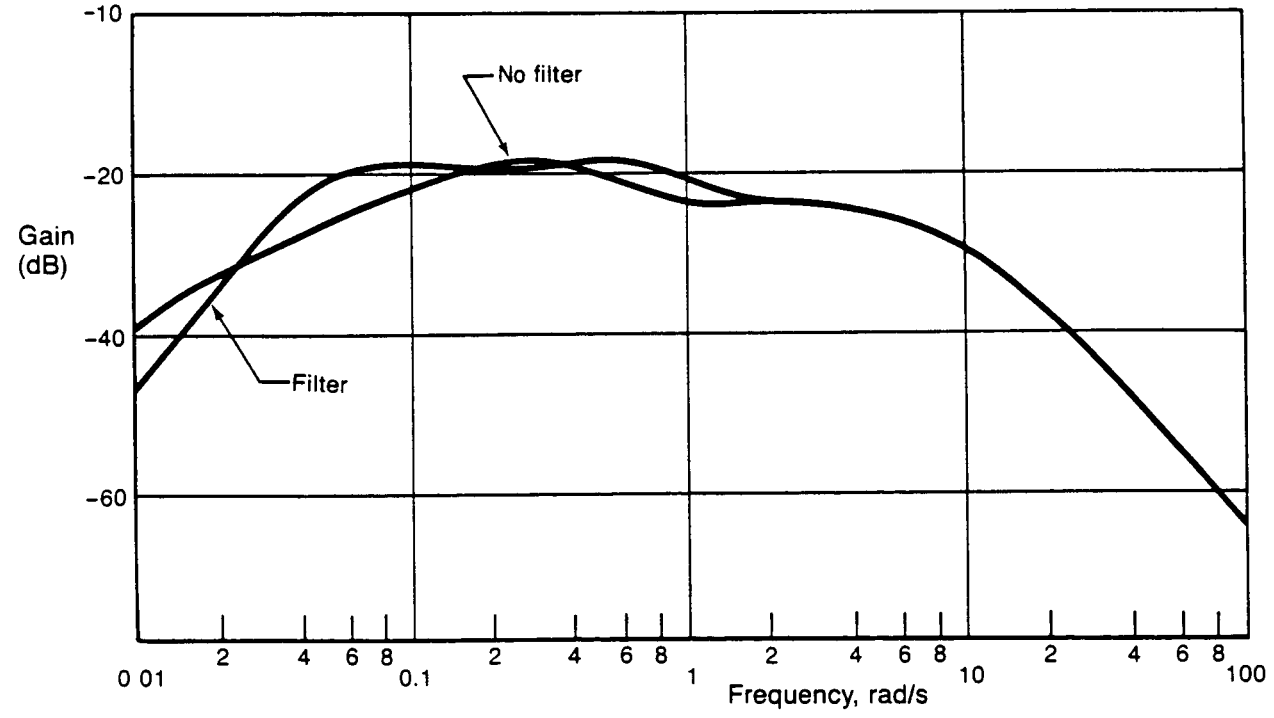

Figure 31. Frequency Response of Elevator $\delta_{e/u}$ (deg) (With and Without Complementary Filter) (Low Speed)

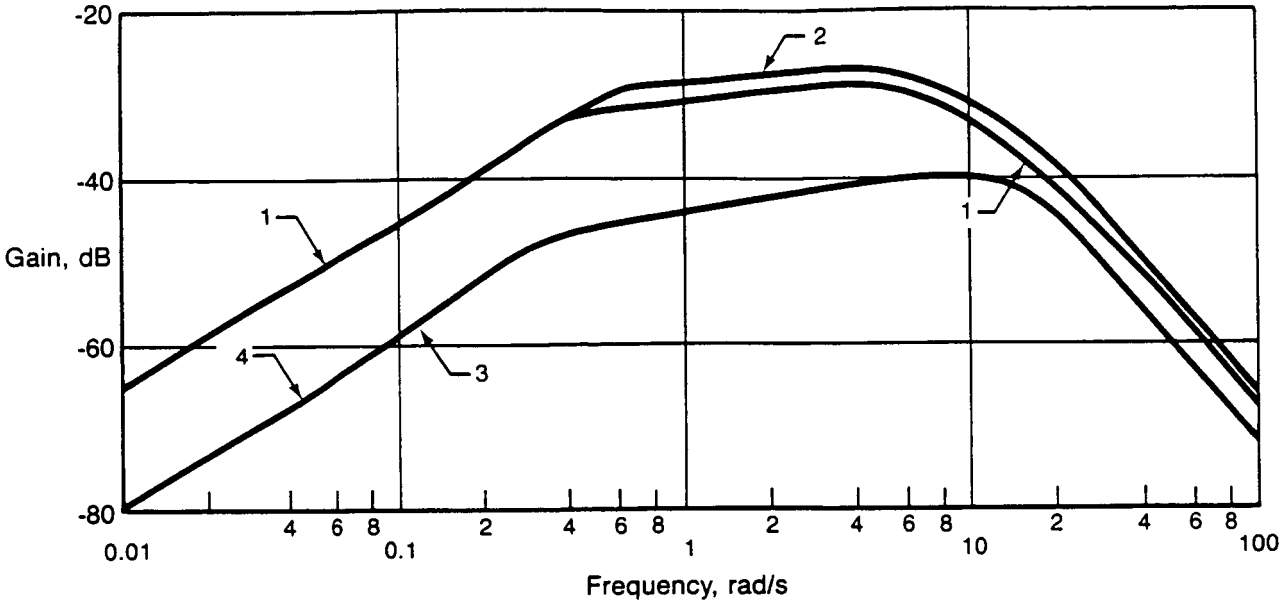

1 Low speed, no filter
2 Low speed, filter
3 High speed, no filter
4 High speed, filter

Figure 32. Elevator Frequency Response in Vertical Turbulence

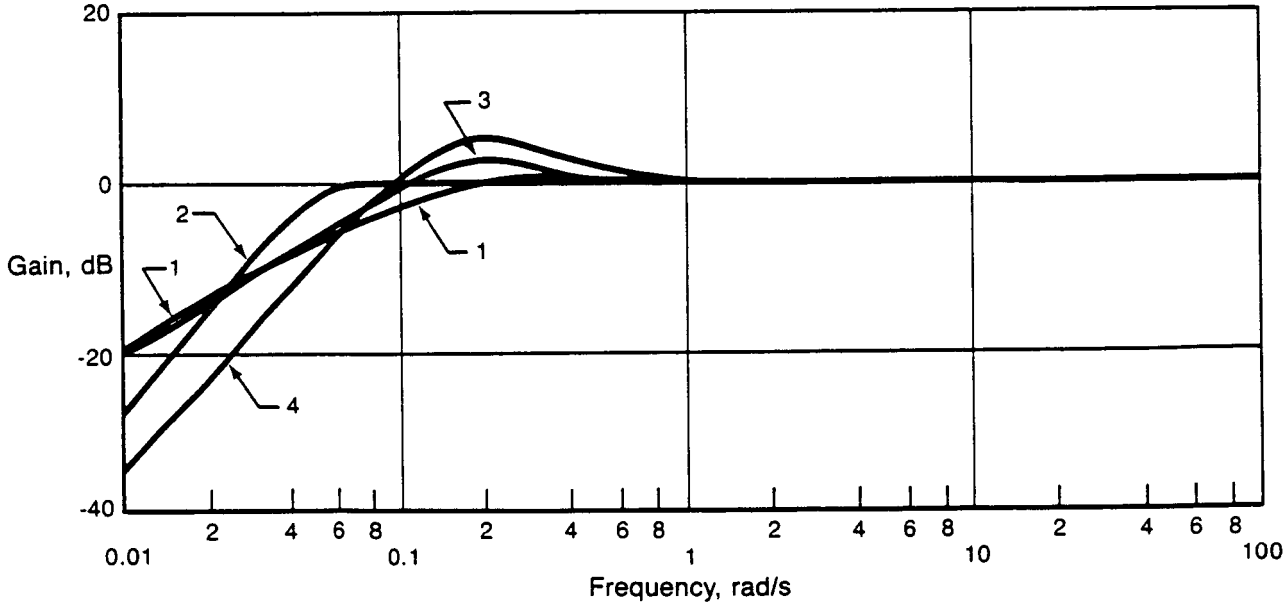

1 Low speed, no filter
2 Low speed, filter
3 High speed, no filter
4 High speed, filter

Figure 33. Airspeed Error Frequency Response in Longitudinal Turbulence

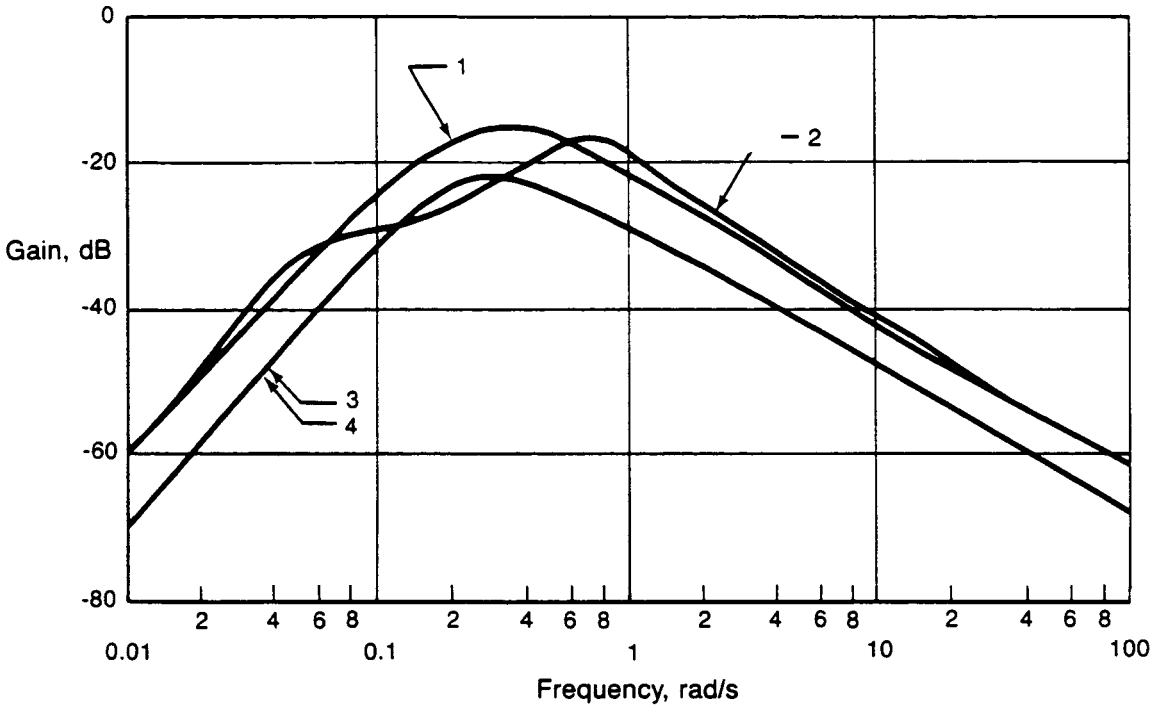

1 Low speed, no filter
2 Low speed, filter
3 High speed, no filter
4 High speed, filter

Figure 34. Airspeed Error Frequency Response in Vertical, Turbulence

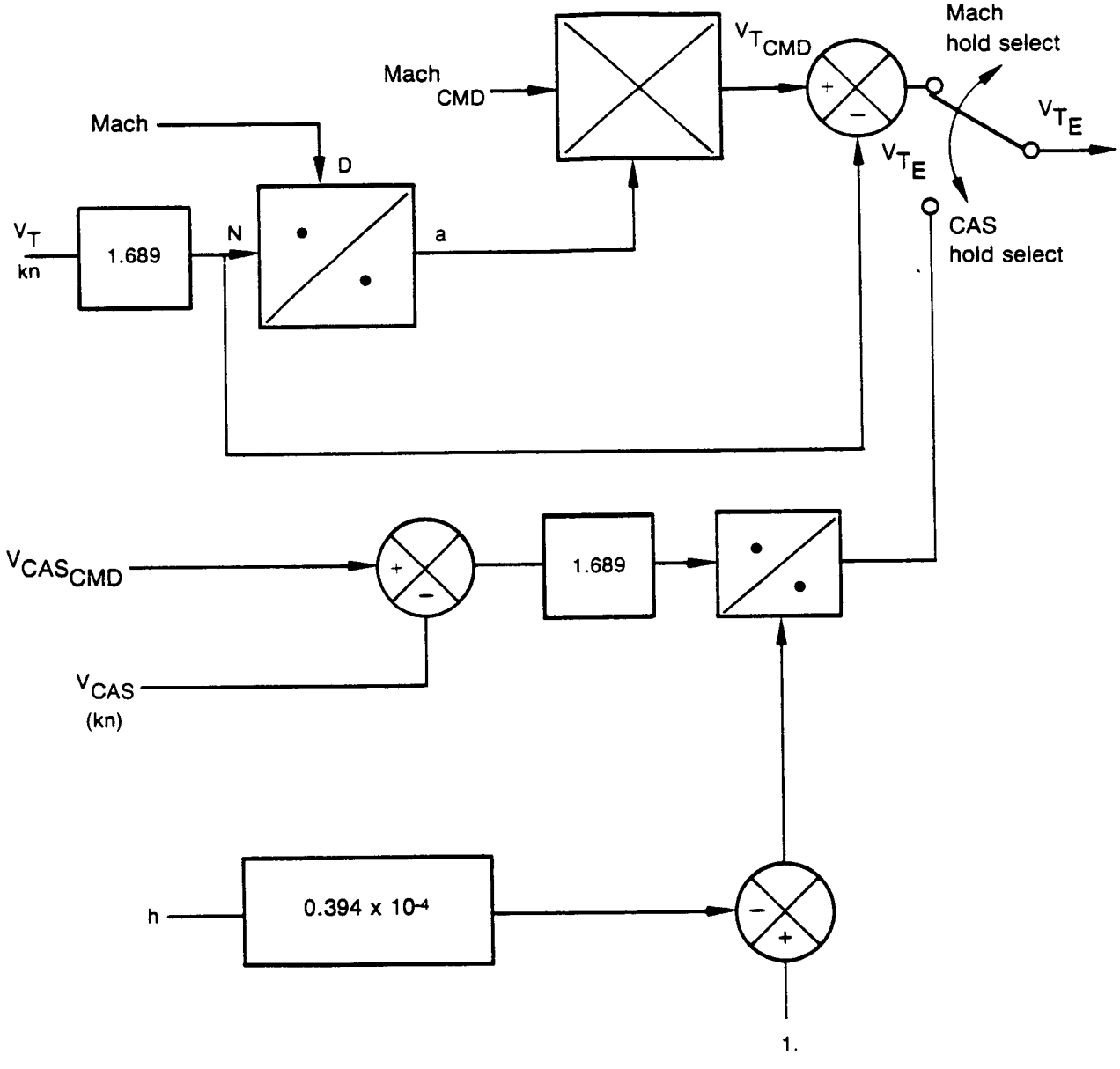

Figure 35. Implementation of Mach/CAS Hold

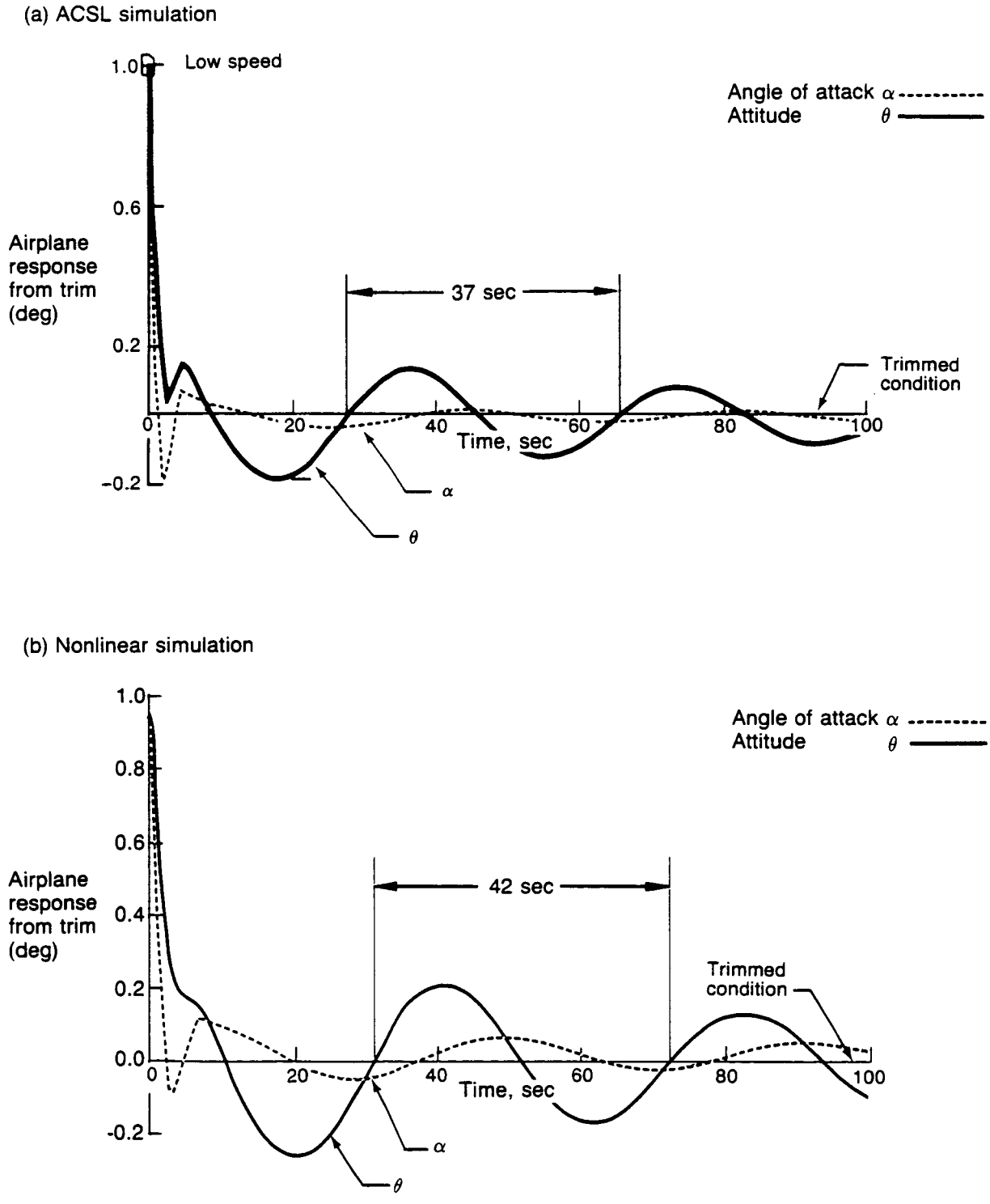

Figure 36. Transient Response of Free Aircraft (1-deg Initial Offset on α and θ) (Low Speed)

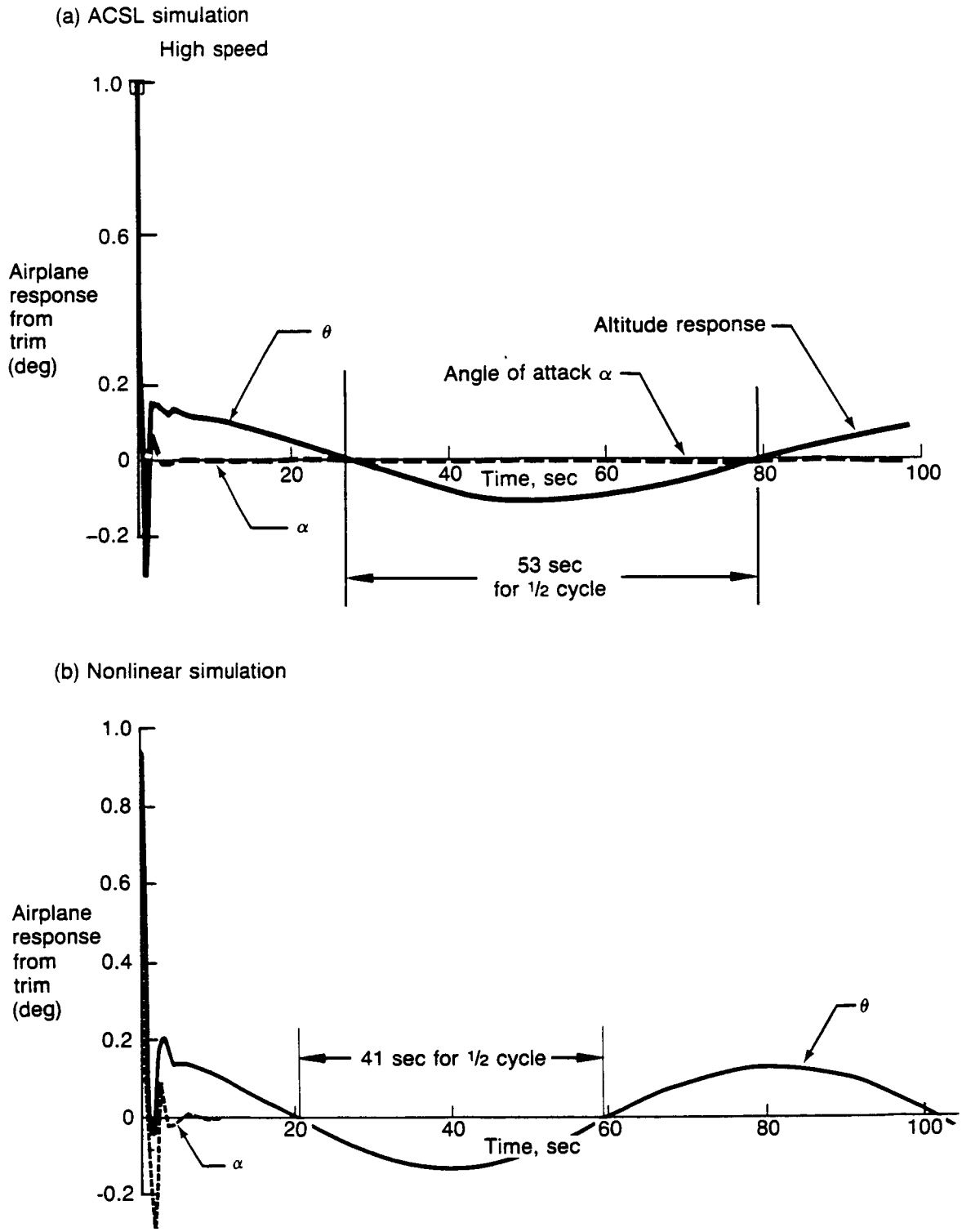

Figure 37. Transient Response of Free Aircraft (1-deg Initial Offset on α and θ) (High Speed)

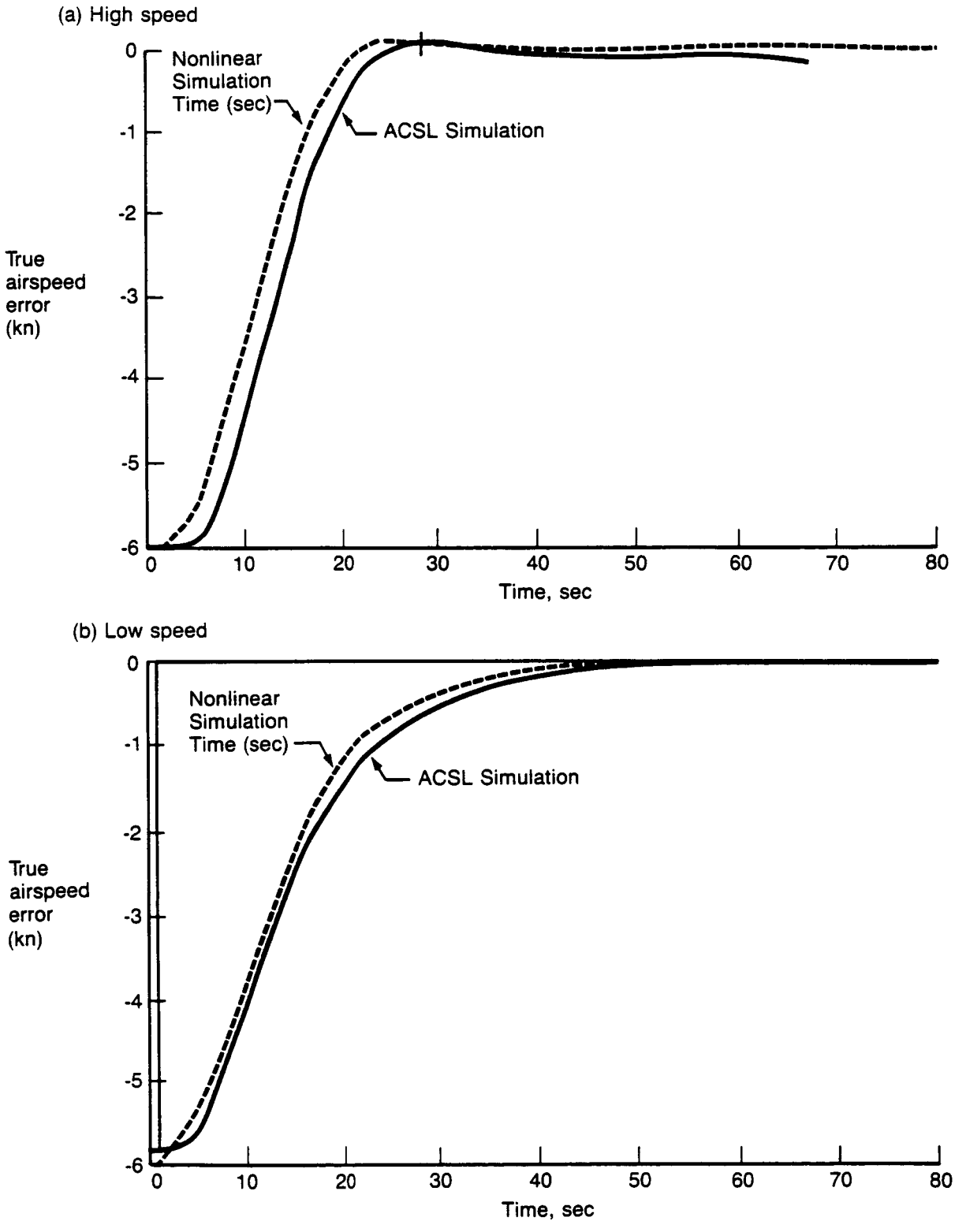

Figure 38. Step Response of Velocity Hold Loop

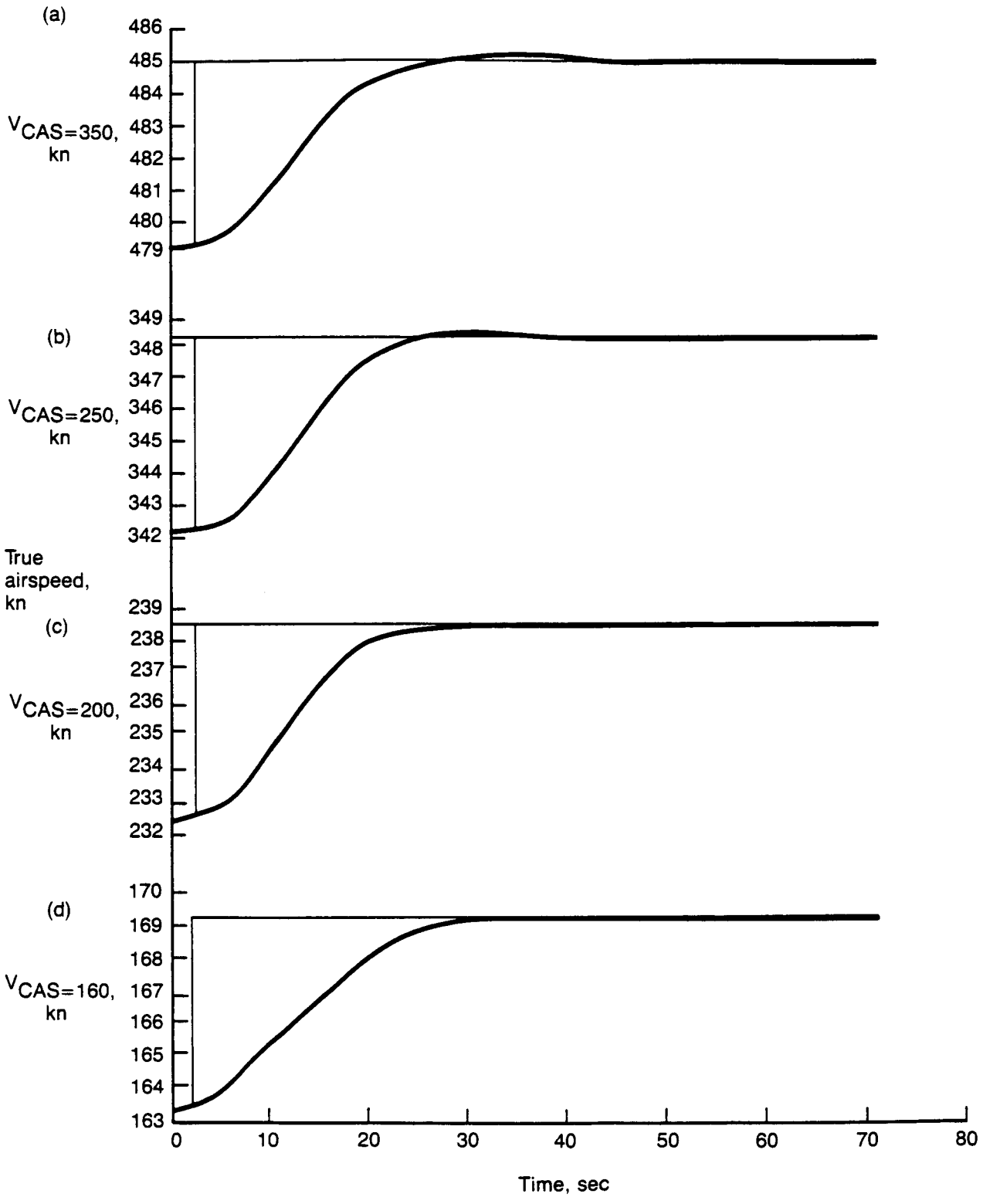

Figure 39. Step Response (Nonlinear Aircraft Simulation)

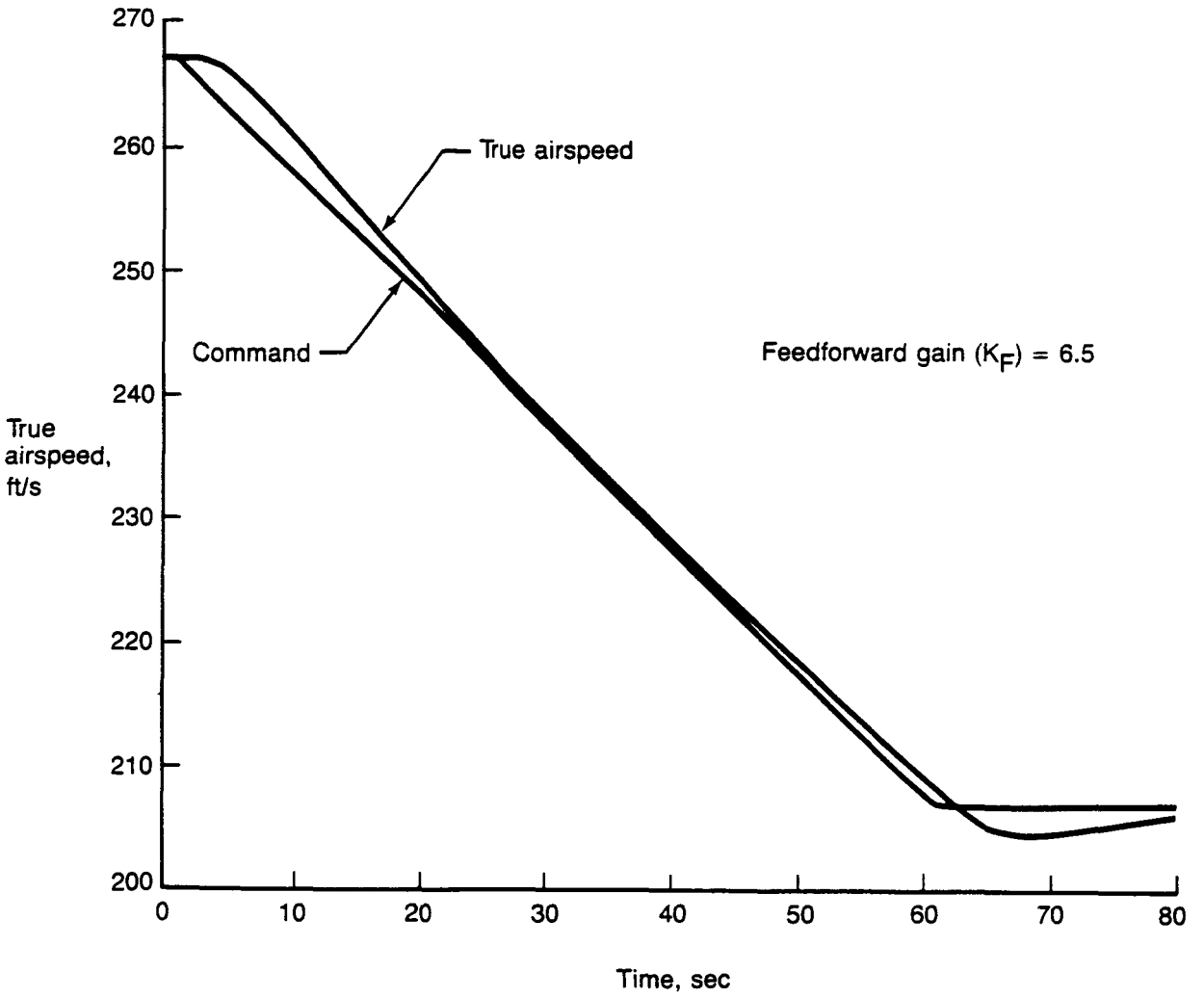

Figure 40. Ramp Response Low Speed (Nonlinear Simulation)

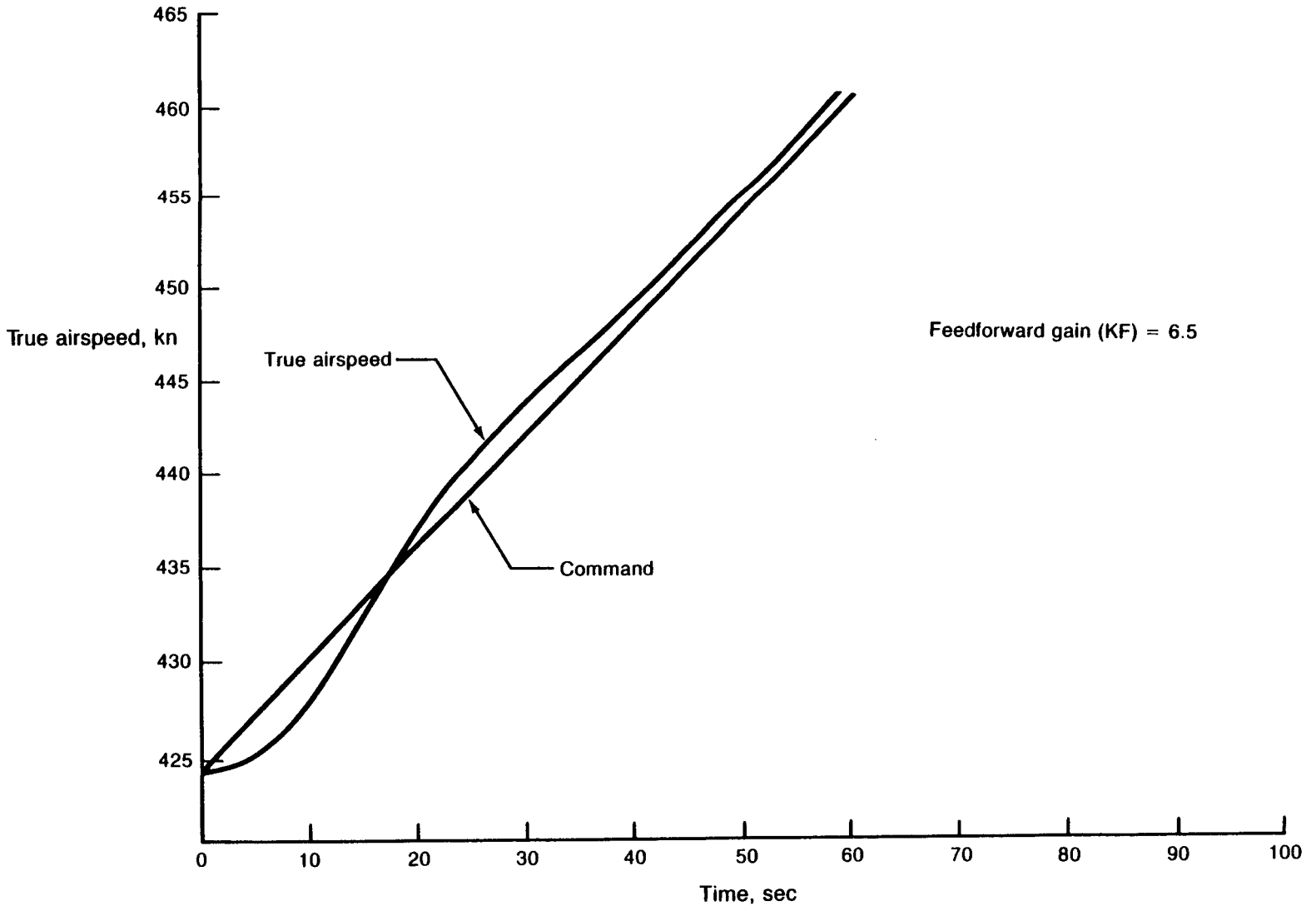

Figure 41. Ramp Response High Speed (RFSL Simulation)

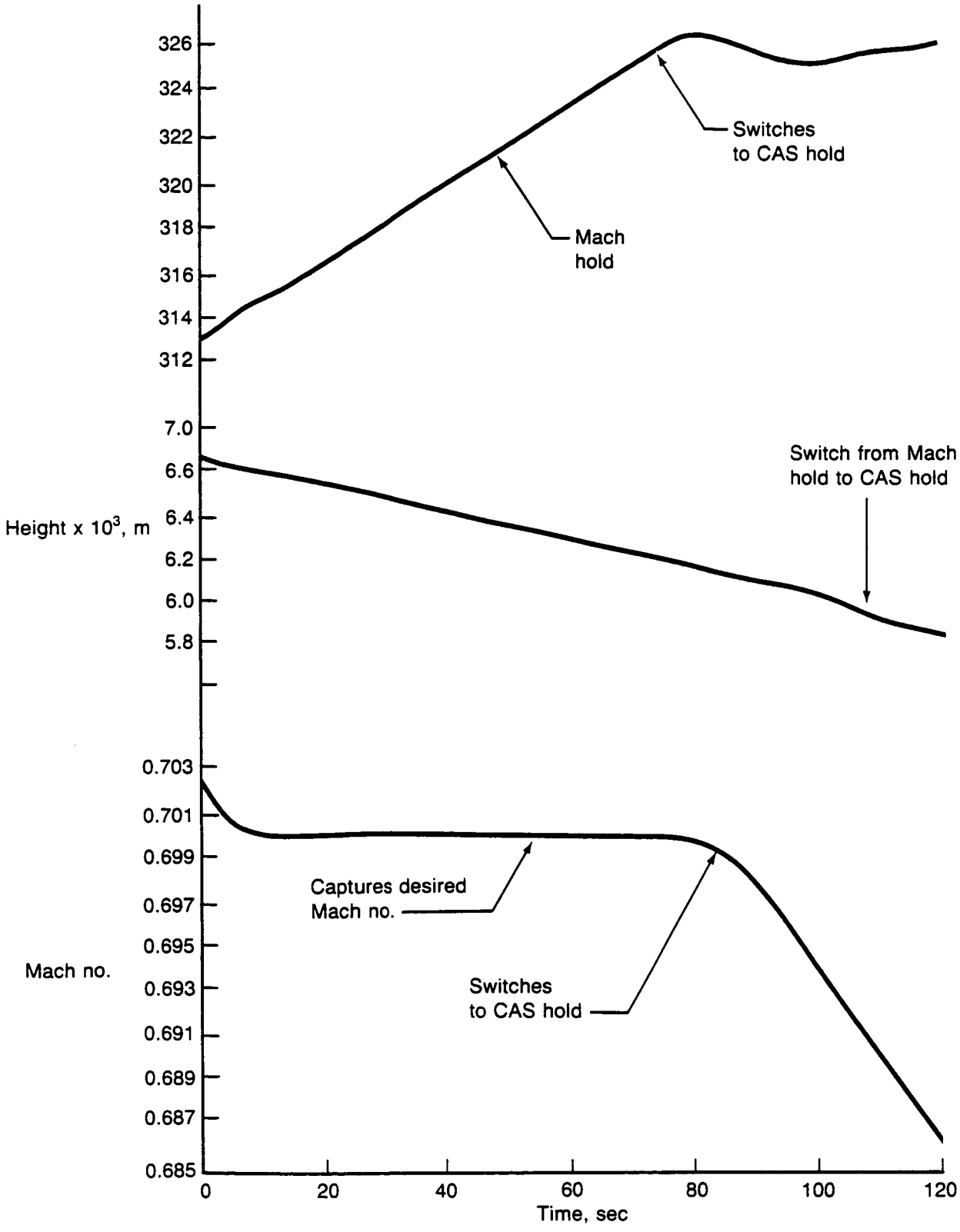

Figure 42. Mach Hold to CAS Hold Aircraft Descent

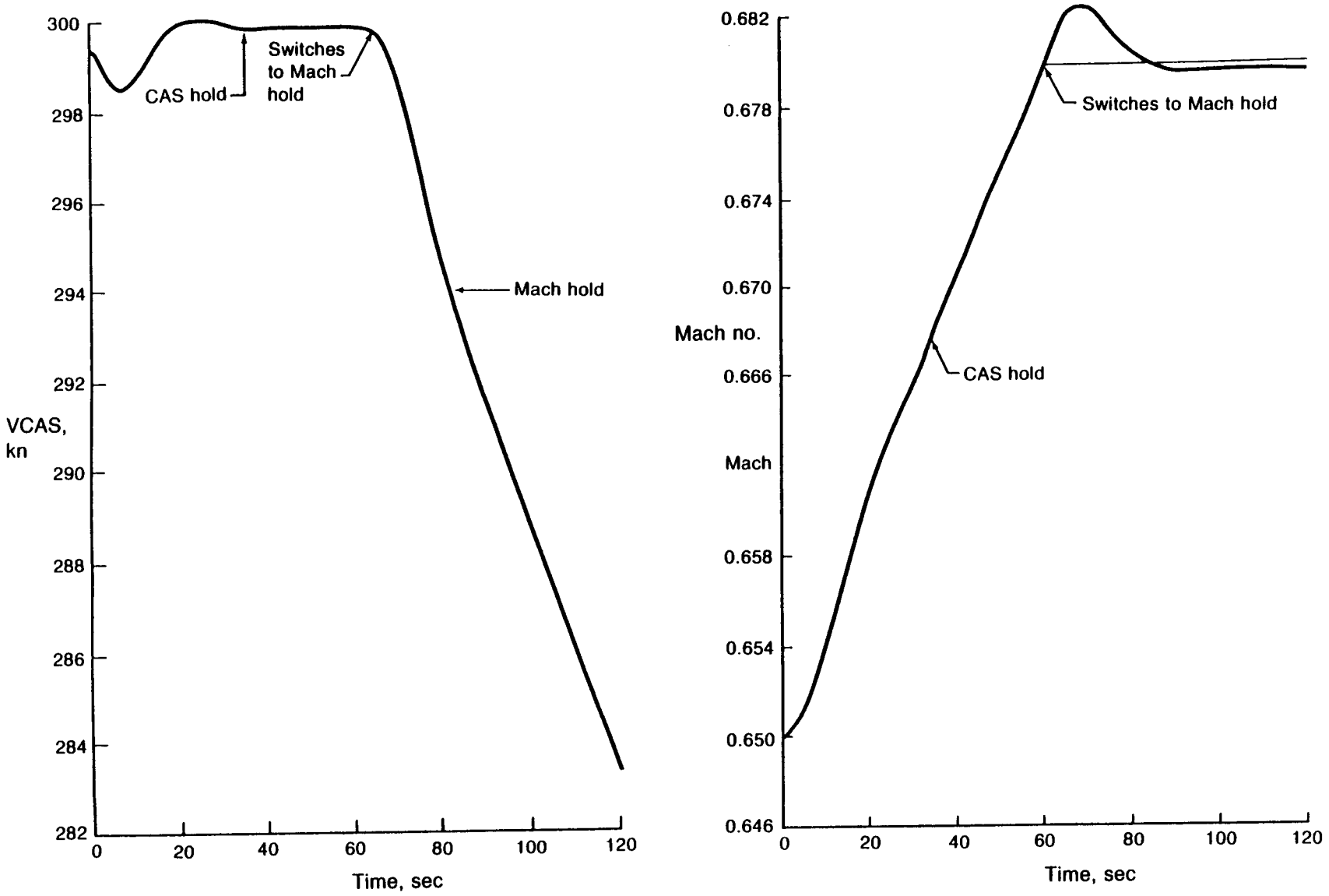

Figure 43. Ascent: CAS Hold to Mach Hold

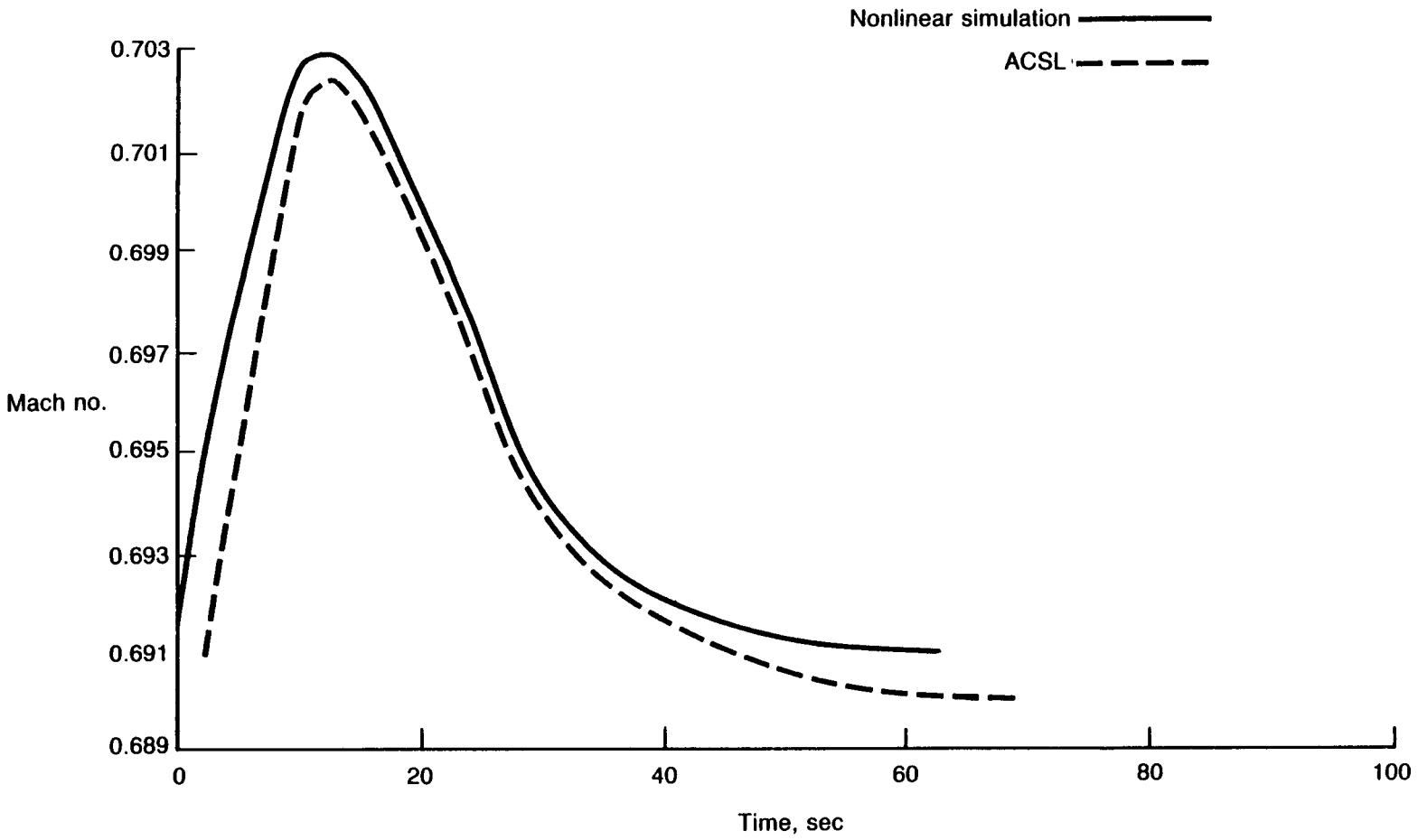

Figure 44. Effect of 1-kn/s Wind Shear (Nonlinear Simulation and ACSL)

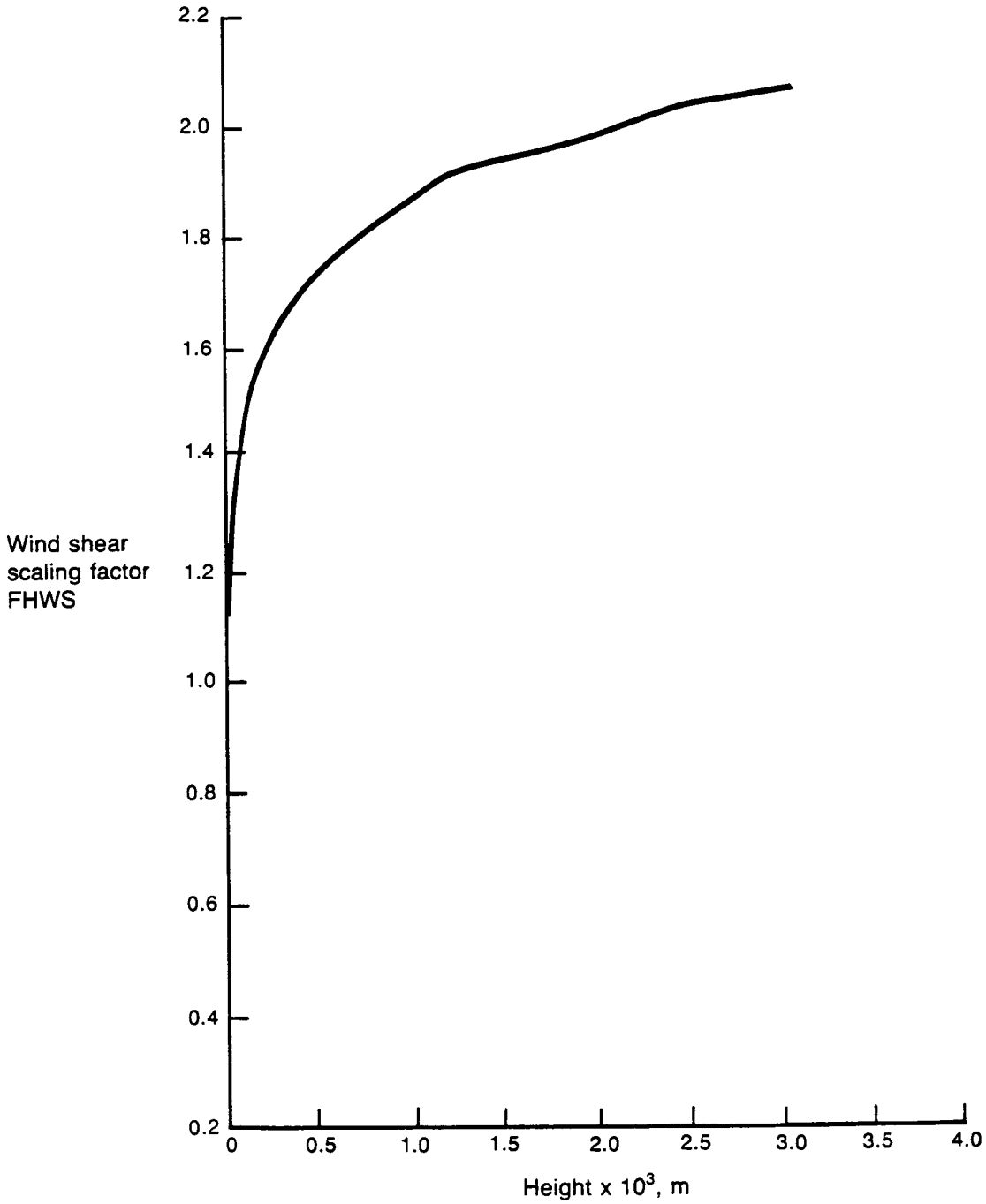

Figure 45. Plot of Wind Shear Scaling Factor FHWS Versus Height

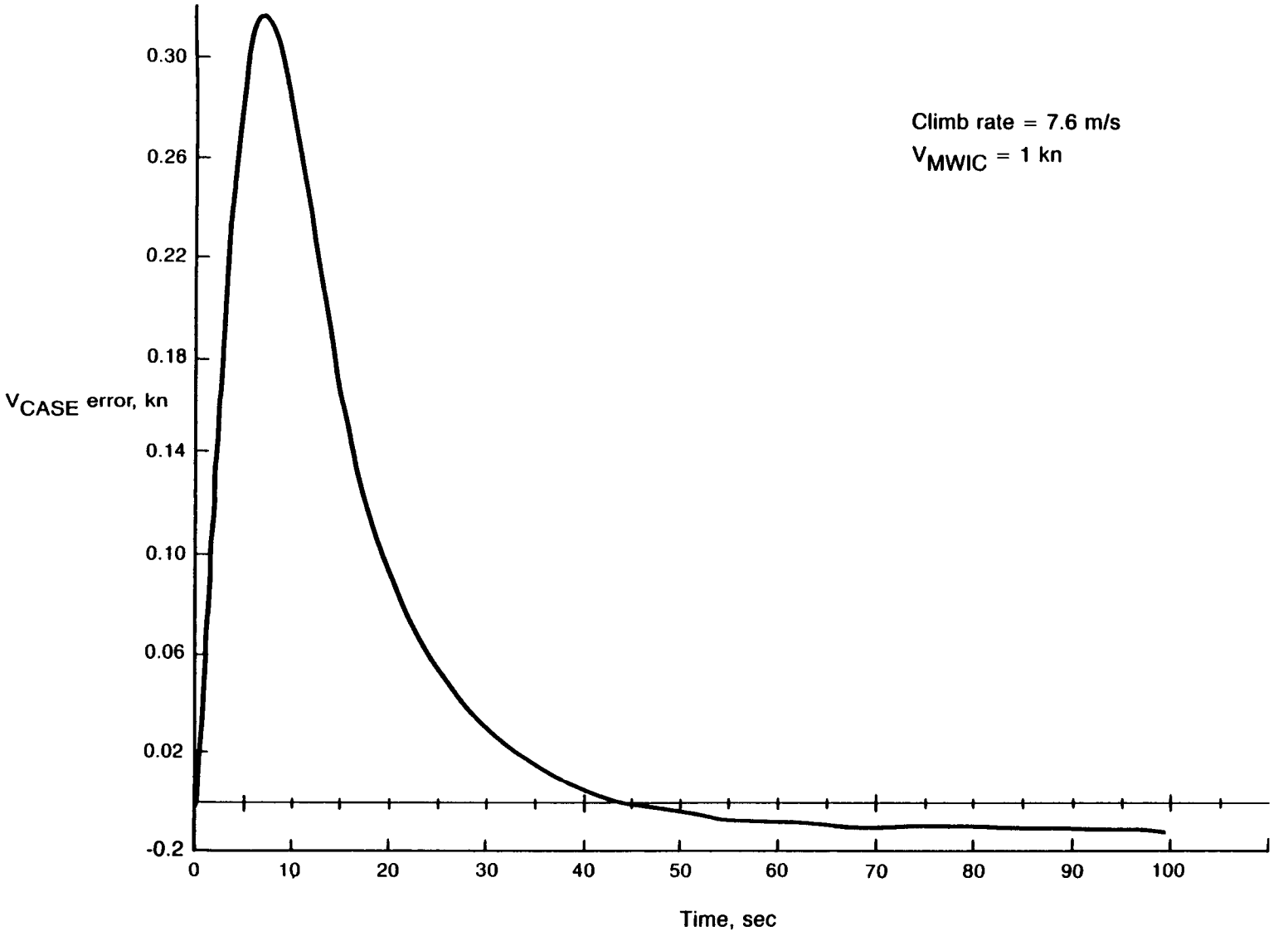

Figure 46. Effect of Wind Shear on Velocity (Low Speed)

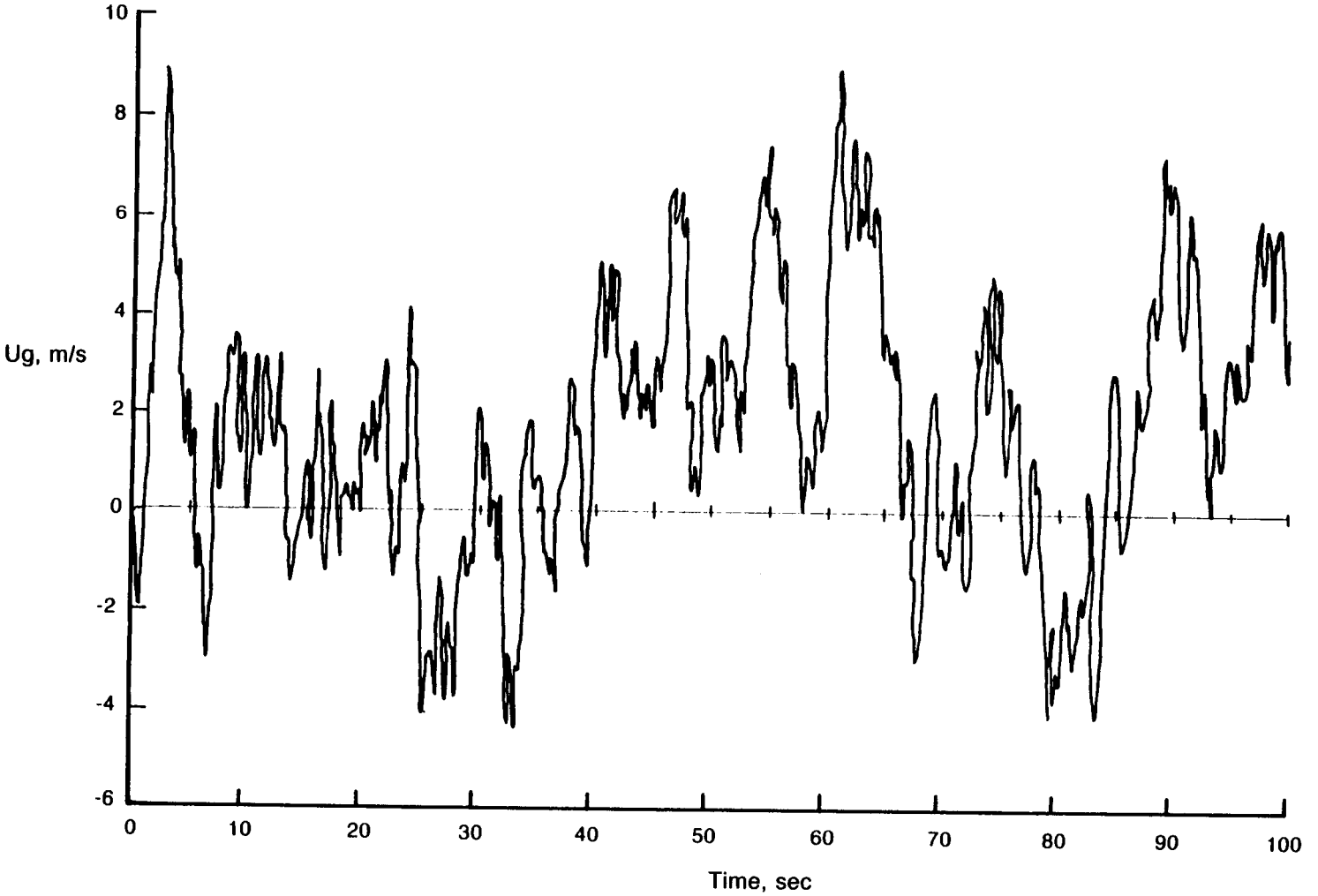

Figure 47 Typical Gust Sample Nonlinear Simulation) Low-Speed Lu = 183M σ_u = 1.5 m/s RMS

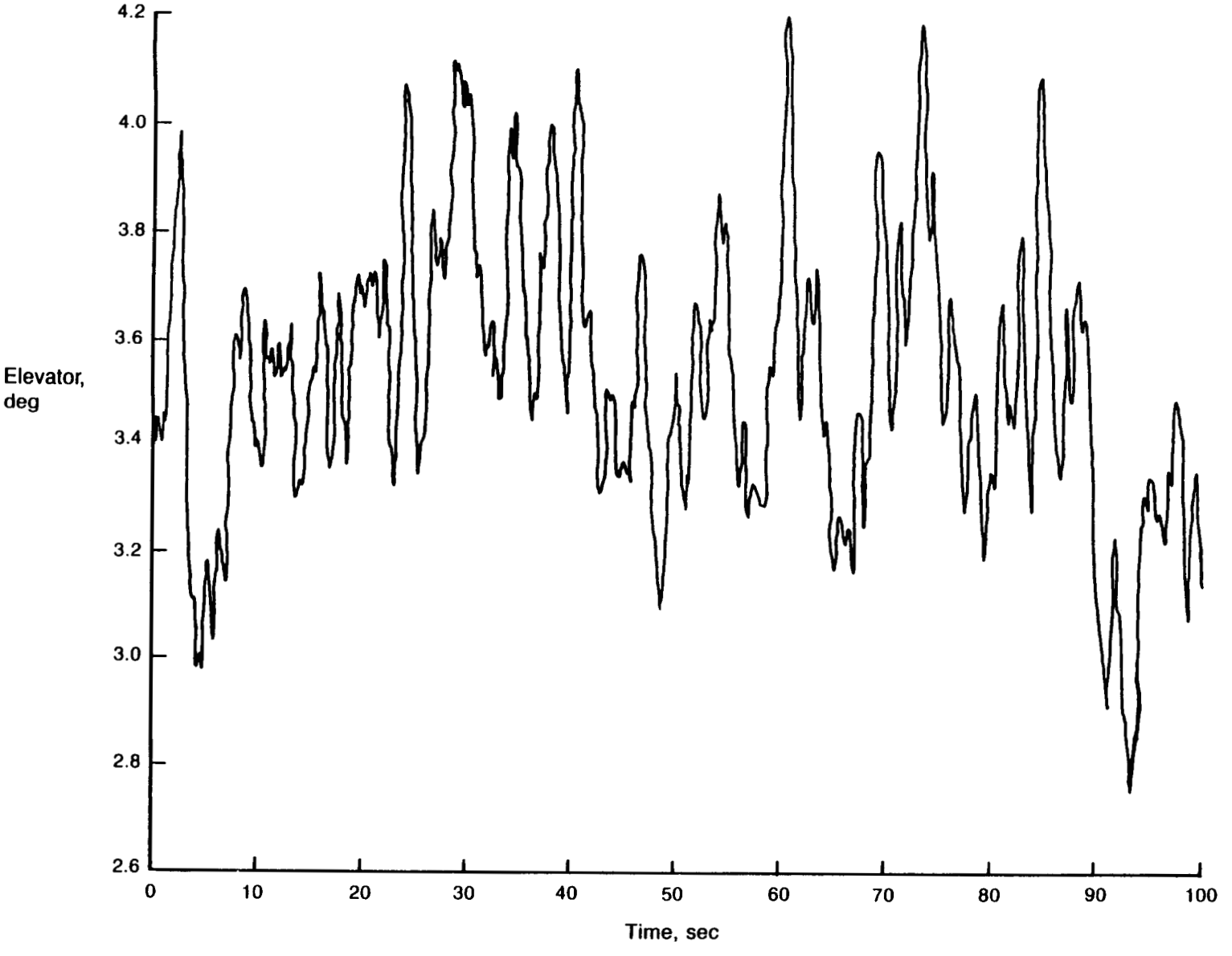

Figure 48. Effect of Gust Sample on Elevator (for Gust Sample as in Fig. 56)

1. Report No.	2. Government Accession No.	3. Recipient's Catalog No.
NASA CR-178029		

4. Title and Subtitle	5. Report Date
Design and Verification by Nonlinear Simulation of a Mach/CAS Control Law for the NASA TCV B737 Aircraft	December 1986
	6. Performing Organization Code
7. Author(s)	8. Performing Organization Report No.
Kevin R. Bruce	
9. Performing Organization Name and Address	10. Work Unit No.
Boeing Commercial Airplane Company P.O. Box 3707 Seattle, WA 98124	11. Contract or Grant No. NAS1-14880
	13. Type of Report and Period Covered
12. Sponsoring Agency Name and Address	Final Report
NASA Langley Research Center Hampton, VA 23665	14. Sponsoring Agency Code

15. Supplementary Notes

NASA Technical Monitor:	Dr. J. F. Creedon
Boeing Technical Supervision:	A. A. Lambregts
Boeing Contract Manager:	R. L. Erwin

16. Abstract

A Mach/CAS control system using an elevator was designed and developed for use on the NASA TCV B737 aircraft to support research in profile descent procedures and approach energy management.

The system was designed using linear analysis techniques primarily. The results were confirmed and the system validated at additional flight conditions using a nonlinear 737 aircraft simulation. All design requirements were satisfied.

17. Key Words (Suggested by Author(s))	18. Distribution Statement
Flight Control System Mach/CAS Control System Profile Descent Procedure Nonlinear Simulation	Unclassified-Unlimited

19. Security Classif. (of this report)	20. Security Classif. (of this page)	21. No. of Pages	22. Price
Unclassified	Unclassified		

FORM 00005